Universitetet i Stavanger

Faculty of Science and Technology

MASTER'S THESIS

Study program/ Specialization: Cybernetics/ Control Engineering	Spring semester, 2013 Open
Writer: Ingeborg Siem Knudsen	…… (Writer's signature)
Faculty supervisor: Tormod Drengstig Second supervisor: Kristian Thorsen	
Title of thesis: **Comparative analysis of mathematical models describing glucose-insulin regulation in vivo**	
Credits (ECTS): 30	
Key words: Biochemical modeling Glucose-insulin regulation Homeostatic control	Pages: 81 + enclosure: 18 Stavanger, 17/06-2013 Date/year

Comparative Analysis of Mathematical Models Describing Glucose-Insulin Regulation in Vivo

Ingeborg Siem Knudsen

Master Thesis

Acknowledgements

The motivation for writing this thesis within the field of biochemical modeling has primarily been my interest in medical technology. Combining principles of process control with anatomy and biochemistry is a very interesting scientific field. A field that illustrates the validity of control engineering outside the strictly industrial context.

I would like to thank my advisor Tormod Drengstig for his guidance and assistance. As the field of biochemistry and anatomy was relatively unknown for me prior to this research work, his assistance regarding the theory and biochemical modeling has been valuable. Furthermore, I would like to thank my second supervisor Kristian Thorsen for assisting me throughout this process.

I would also like to express my gratitude to my family. My mother Kristin Siem Knudsen for encouragement and loving support. My sister Victoria Siem Knudsen *cand. med.* who has inspired me to write a thesis related to medical technology. And my two brothers, Bjørn and Greger Siem Knudsen, for their encouragement.

Ingeborg Siem Knudsen
Stavanger, June 2013

Abstract

In this thesis, mathematical models describing glucose-insulin regulation within the human body have been studied. Glucoregulatory models are valuable in diabetes related research. Monitoring glucose-insulin dynamics, testing software and hardware related to autonomous insulin infusion, medical testing and student training, are some of the main motivating factors for developing physiologically accurate glucoregulatory models. In addition, mathematical modeling of glucose control demands that the anatomical process is studied in detail, which can increase our understanding of the process itself. This can in turn improve the medical service for diabetic patients. This thesis presents and evaluates the anatomical validity of six glucoregulatory model. The evaluation will focus on the models' ability to simulate a physiologically plausible glucose-insulin dynamics, both quantitatively and qualitatively. Homeostatic glucose control will also be a central focus point when evaluating the models' simulation performance. Based on this evaluation, improvements and modifications are suggested.

This thesis is primarily a theoretical study, made up of three main segments. The first segment will present the theoretical research conducted regarding anatomy, biochemistry, and biochemical modeling. The second segment is a presentation of all the six glucoregulatory models studied. The third will present and evaluate the Matlab and Simulink simulation result, and present a optimized model based on the model study.

Contents

1 Introduction **6**
- 1.1 Problem to be addressed . . . 6
- 1.2 Background . . . 6
- 1.3 Anatomy . . . 7
  - 1.3.1 Enzymes . . . 7
  - 1.3.2 The pancreas . . . 8
  - 1.3.3 Homeostasis . . . 9
  - 1.3.4 The glucose-insulin regulatory system . . . 9
  - 1.3.5 Diabetes . . . 11
- 1.4 The developement within biochemical modeling . . . 13
- 1.5 Thesis outline . . . 14

2 Enzyme kinetics and biochemical modeling **16**
- 2.1 Biochemical reactions and enzyme kinetics . . . 16
- 2.2 Michaelis-Menten equation . . . 19
- 2.3 Inhibition . . . 20
- 2.4 Controller motifs . . . 21
- 2.5 Modeling homeostatic control . . . 24
- 2.6 Model classification . . . 26
- 2.7 Model development . . . 26

3 Models of the glucoregulatory system **29**
- 3.1 Choice of models . . . 29
- 3.2 The BMM . . . 31
  - 3.2.1 Glucose dynamics . . . 32
  - 3.2.2 Insulin dynamics . . . 32
  - 3.2.3 Remote insulin in action . . . 33
  - 3.2.4 Complete model . . . 33
- 3.3 The βIG-model . . . 35
  - 3.3.1 Glucose dynamics . . . 36
  - 3.3.2 Insulin dynamics . . . 36

3.3.3 β-cell mass dynamics . . . 37
3.3.4 Complete model . . . 38
3.4 The βIGIR-model . . . 39
3.4.1 Glucose dynamics . . . 40
3.4.2 Insulin dynamics . . . 40
3.4.3 The dynamics of insulin receptors . . . 41
3.4.4 Complete model . . . 41
3.5 The GIE-model . . . 43
3.5.1 Glucose dynamics . . . 44
3.5.2 Insulin dynamics . . . 45
3.5.3 Glucagon dynamics . . . 45
3.5.4 Complete model . . . 46
3.6 The S&H-model . . . 49
3.6.1 Glucose dynamics . . . 49
3.6.2 Insulin dynamics . . . 50
3.6.3 Complete model . . . 51
3.7 The GIM-model . . . 52
3.7.1 GUI-presentation . . . 52

4 Implementation and results **57**
4.1 Implementation . . . 57
4.2 Glucose/Insulin response . . . 61
4.2.1 The GIM-model . . . 64
4.2.2 The Bergman Minimal Model . . . 65
4.2.3 The βIG-model . . . 66
4.2.4 The βIGIR-model . . . 67
4.2.5 The GIE-model . . . 68
4.2.6 The S&H-model . . . 69
4.3 Homeostasis . . . 71
4.3.1 The BMM . . . 73
4.3.2 The βIG- and βIGIR- model . . . 74
4.3.3 The GIE- and S&H-model . . . 76
4.4 Model optimization . . . 77

5 Discussion and conclusion **80**
5.1 Conclution . . . 80
5.2 Further work . . . 81

A Content of CD **87**

B Exogenous glucose infusion **88**

C Model Implementation In Simulink **90**
C.1 Input Signal 90
C.2 The BMM 92
C.3 The βIG-model 93
C.4 The βIGIR-model 94
C.5 The GIE-model 95
C.6 The S&H-model 96

D Source Code **97**
D.1 Simulating And Ploting Glucose/Insulin Response 98
D.2 Simulating And Ploting "Homeostasis Test" 105

Chapter 1

Introduction

1.1 Problem to be addressed

To study and compare a set of mathematical models describing glucose-insulin control. The study will be focused on examining the models' glucose-insulin oscillation related to food intake, and to examine their ability to simulate homeostatic glucose control.

1.2 Background

Industrial controllers are the building blocks of control engineering. Even though the human body does not contain controllers in the traditional, industrial sense, the principles of control engineering is highly valid and applicable for biochemical regulatory processes. Mathematical modeling of these processes within the human body has been a subject for scientific research for over a century. This way of describing anatomical, physiological and biochemical processes has led to an increased understanding of the human regulatory system, the same way as the principles of control engineering has contributed markedly to the development and scientific innovation in numerous other engineering fields [24]. Examples of these are process automation and -control, subsea technology and medical engineering.

1.3 Anatomy

1.3.1 Enzymes

Chemical reactions within living organisms are crucial for the maintenance of life. Examples of such reactions are nutrition uptake from food, utilization and distribution of water in cells, reaction related to our immune system, regulation regarding pH-level, blood sugar and -salt concentration [6]. These reactions are mostly carried out spontaneously, though some of them require *catalyst* for them to initiate or be carried out fast enough. Catalyst are substances present in chemical reaction, speeding up the reaction rate to up to more than a million times, compared with the uncatalyzed reaction [20]. Catalysts are able to work as reaction accelerators without themselves being permanently altered in the process [20]. Catalysts are reusable as they return to their initial state after the reaction has been carried out.

Biochemical catalysts are mostly proteins called *enzymes* [20]. The glucoregulatory process is dependent of these enzymes as they lower the energy demand of certain biochemical reaction, enabling them to be carried out spontaneously [20]. The enzymes in focus when considering the glucoregulatory process are the hormones *insulin* and *glucagon*. These hormones are responsible for the regulation of blood levels of triglycerides, glucose, fat- and amino acids, as well as the management of tissue metabolism [6].

Insulin is responsible for the lowering and stabilizing of an elevated blood glucose concentration related to food intake [6]. This is done by accelerating the glucose-uptake in skeletal muscle and fat, combined with an inhibition of the glucagon secretion. Opposite to insulin, the hormone glucagon elevates the lowered glucose concentration experienced while fasting, exposed to physical stress or -exercise. The stored glucogen is then converted into glucose, a hepatic reaction catalyzed by the enzyme glucagon [6]. Figure 1.1 illustrate computer generated molecule images of these hormones.

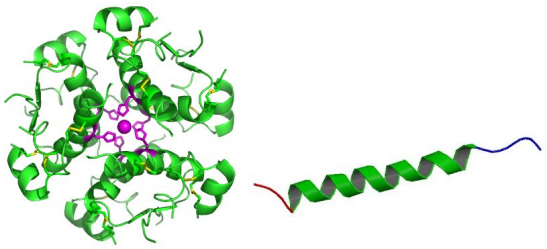

Figur 1.1: Insulin and glucagon molecule respectively [25, 26].

1.3.2 The pancreas

Insulin and glucagon are hormones secreted from the *pancreas* - an organ with a vital role in the glucoregulatory process. The pancreas is a glandular organ located in the central abdomen, see figure 1.2.

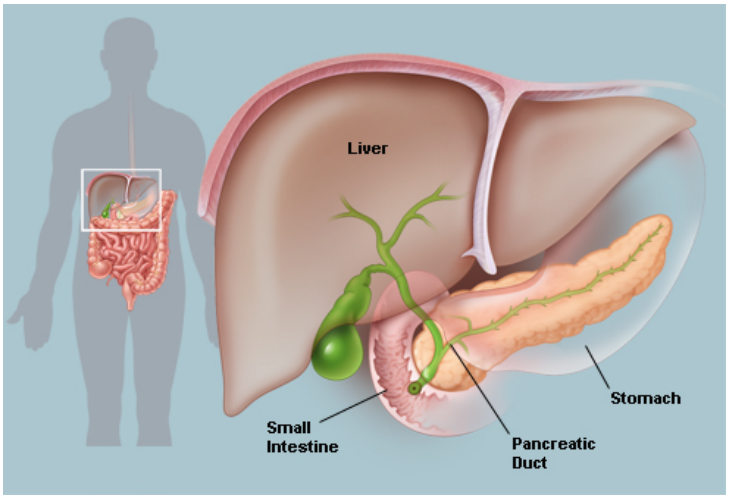

Figur 1.2: An illustration of the pancrease and its location in the abdomen [28].

The primary functions of the pancreas are to contribute to digestion in the small intestine, and act as a endocrine gland secreting hormones [27]. The organ comprises two types of tissue, namely dark-staining cells related to the digestion process, and lighter-stained cell-clusters called the *Islet of Langerhans* [27]. In this report, we will focus on the latter.

The Islet of Langerhans are pancreatic regions discovered by Paul Langerhans, a German pathological anatomist, in 1869 [16]. The Isle of Langerhans are the endocrine regions[1] of the organ. In the least, five types of cells inject the secreted hormones directly into the blood stream. Examples of such cell types are α- and β-cells that secrete the previously mentioned hormones glucagon and insulin respectively.

Having introduced insulin, glucagon and the pancreas, we will now present their interaction in the glucose-insulin regulatory system.

[1] Hormone producing regions.

1.3.3 Homeostasis

Every day, the human body is exposed to, and affected by external and internal perturbations. These perturbations affect the biochemical processes and dynamic functions within the human body. Counteraction of, and compensating for these disturbances to maintain internal stability, *homeostasis*, is done through thoroughly regulation and control. The term homeostasis was introduced by the American physiologist Walter Cannon (1871–1945), and is a fusion of the words *homeo* and *stasis* meaning "the same" and "standing or staying" respectively [5]. There are many bodily functions that require homeostatic control. Examples of these are the regulation of plasma glucose concentration, body temperature, pH-level, ion-concentration as well as our balance- and visual system [5]. A too strong deviation form homeostatic normal values, caused by a defect in the homeostatic control, can lead to severe, and potentially life threatening conditions.

1.3.4 The glucose-insulin regulatory system

The glucose-insulin regulatory system is kept under tight homeostatic control. Glucose is the human cells primary source of energy and is delivered to the cells through the blood stream. For the cell to have adequate access to glucose, the glucose level in the blood stream needs to be kept within a certain range[2]. The glucose-insulin regulatory system regulates the plasma glucose level, keeping the levels within this range [6]. The main contributor for maintaining plasma glucose homeostasis is the earlier mentioned *pancreas,* and the two hormones *insulin* and *glucagon*.

The digestion of, and nutrition uptake from food will lead to an elevation of the blood sugar level. This elevation will break the blood sugar homeostasis and the body will try to oppose this change. When the blood sugar level exceeds approximately 110 mg/dl, the hormone insulin is secreted from the Islet of Langerhans' β-cells in the pancreas. Insulin accelerates the conversion of the excess glucose in the blood stream into glycogen through a series of kinetic biochemical reactions. Glucogen is stored in the liver, and acts together with stored glucose in muscle and adipose tissue as a long-term energy supply. Through these means, plasma glucose levels are reduced and homeostasis is restored [6].

When the glucose level drops below 70 mg/dl, usually associated with fasting, physical activity or stress, the pancreatic α-cells responds by secreting the hormone glucagon. Glucagon inhibits the glucose-to-glycogen conversion,

[2]Normally 70-110 mg/dl for fasting non-diabetic subjects [6].

and reverse the process. The glucogen stored in the liver is degraded and converted into glucose which in turn is taken up in the blood stream, elevating the glucose level and restoring plasma glucose homeostasis. This regulatory cycle is visually presented in figure 1.3.

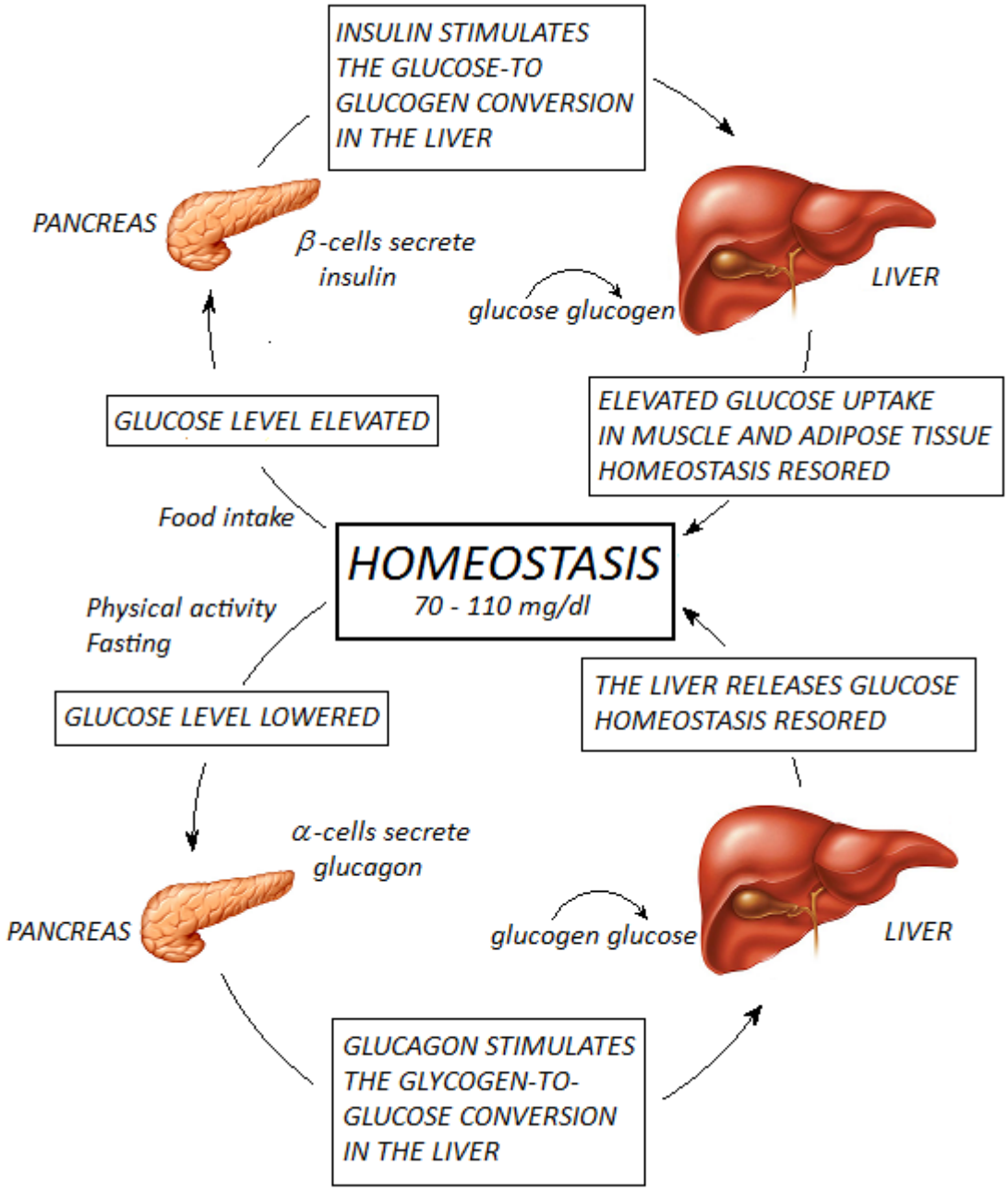

Figur 1.3: The glucose-insulin-glucagon regulatory system [8].

Figure 1.3 illustrate the general steps of maintaining blood-sugar homeostasis [3]. Some people are challenged or inhibited to naturally maintain this equilibrium, namely diabetics.

1.3.5 Diabetes

"Diabetes mellitus describes a metabolic disorder of multiple etiologies characterized by chronic hyperglycemia with disturbance of carbohydrate, fat and protein metabolism resulting from defects in insulin secretion, insulin action or both."[4] According to The Norwegian Institute of Public Health, in 2012 there were 375,000[4] people in Norway suffering from diabetes [1]. Patients that suffer from diabetes are unable to regulate their blood sugar level naturally when the homeostasis is broken. The condition is divided into two groups; diabetes type 1 and diabetes type 2. In both cases, the subjects' blood sugar level is too high, potentially leading to life threatening condition if not treated.

Diabetes type 1[5], also called insulin-dependent or juvenile-onset diabetes, affects among 10% of the total number of patients diagnosed with the condition [11]. Type 1 diabetes is commonly diagnosed through detection of symptoms such as increased hunger and/or thirst, weight loss, frequent urination, dry mouth and fatigue [12]. In contrast to diabetes type 2, DMT1 is not a result of poor dieting or overweight, but has a stronger connection to genetics.

Subjects diagnosed with type 1 diabetes have been subjected to an autoimmune attack of the pancreatic β-cells, causing relative or total inhibition if insulin secretion. The reduction in, or absent of insulin supply inhibits the plasma glucose regulatory process to lower blood sugar level, a condition that can be fatal [12].

Being a chronic condition, diabetes needs to be treated carefully for the subjects to live close to normal lives. Since the pancreas is unable to produce insulin, this hormone has to be artificially injected to maintain glucose regulation, hence the name insulin-dependent. Insulin replacement therapy involves a manually insulin injection, demanding close monitoring of the glucose level using a glucose meter [12]. Alternatively, a insulin pump is used for the insulin injections. In more critical cases, Islet cell- or complete pancreas transplantation are preformed to restore glucose regulation. Such treatment

[3] Reference of liver figure: http://www.sccollege.edu/SiteCollectionImages/Private/816_liver.jpg
Reference of pancreas figure: http://www.visualphotos.com/image/1x6346825/human_pancreas

[4] Out of 375,000 diabetic subjects there are 2,500 with type 1 and 350,000 with type 2 diabetes.

[5] Hereby also referred to as DMT1 (diabetes mellitus type 1).

is only preformed when highly necessary as the side effects, complication and risk associated with such a procedure might be greater than the medical benefits gained. In most cases, manually injection of insulin is an adequate method of treatment [12].

Diabetes type 2 [6], also called non-insulin dependent or maternity-onset, affects amount 90% of the total number of patients diagnosed with diabetes [11]. Symptoms include frequent urination, increased thirst and hunger, weight loss, blurred vision, peripheral neuropathy, itchiness and fatigue [13]. In contrast to DMT1, which is a condition that is primarily linked to genetic predisposition, the development of DMT2 is strongly connected to factors related to people's environment and lifestyle. Examples of such factors are obesity[7], stress, lack of exercise and poor dieting. Females and elderly are more likely to develop the condition.

DMT2 differ from diabetes type 1 in that the insulin production is partly of fully functioning. The complication in DMT2 is that subjects have developed a resistance or intolerance of the insulin secreted from the pancreas. The subjects are therefore unable to utilize the insulin in the glucose regulatory process, leading to elevated plasma glucose levels, which further on can lead to serious life threatening conditions [13].

While the treatment of DMT1 is limited to, or focused on recovering pancreatic functionality, treatment of DMT2 is more complex focusing on proactive measures and health promotion [13]. Improvement of diet, exercise level and physical health, medication and even weight loss surgery are measures used to increase insulin sensitivity and -action, and reduce the complications related to DMT2.

If treated right, diabetics can live close to normal lives. If not, the patient is at immediate life threatening risk. Hypoglycemia, or too low blood sugar, is a common condition associated with diabetes. Hypoglycemia can cause mild dysphoria, seizures, unconsciousness, and in some cases permanent brain damage or death [14]. In contrast to hypoglycemia, hyperglycemia is caused by a too high glucose level. Generally, temporary hyperglycemia is a asymptomatic and benign condition. However, subjects experiencing chronic or frequent hyperglycemic episodes over a long time period stand at risk for developing severe, and potentially life threatening complications. Examples of these are kidney disease, cardiovascular damage, neurological damage, impaired vision or blindness and amputation [15].

Diabetes is the result of a malfunction in the glucose control process. Math-

[6] Hereby also referred to as DMT2 (diabetes mellitus type 2).

[7] Body mass index > 30

ematical modeling and analysis of said process can therefor contribute to an increased understanding of the cause and effect of this malfunction, which in turn can improve the medical treatment of the condition.

1.4 The developement within biochemical modeling

Mathematical models of biochemical metabolism have been a subject to research for over 50 years. To consider biochemical processes using the principles of industrial process control has contributed to increased understanding of, and medical development within the field of anatomical process control. The following will focus on models of glucose-insulin dynamics in vivo[8].

Models of the glucoregulatory system can be traced back to 1961 when Victor Bolier [54] presented the first model describing glucose-insulin dynamics related to blood sugar regulation. This was a fairly simple model comprising two linear ordinary differential equation which illustrated the principle of the glucose-insulin interaction [36]. In spite of its simplicity, the model turned out to be the foundation of the work conducted by scientist like Cobelli [58] and Ackerman [55, 56, 57], people considered pioneers within the field of glucoregulatory- and diabetes modeling. Ackerman's et al. models were based on oral glucose tolerance test describing individuals capacity of glucose utilization.

One of the most significant contributions is however considered to be the work conducted by Richard Bergman et al. [59]. His model, known as "The Bergman Minimal Model", is related to his award winning diabetes research. With its simple structure and limited complexity, the model is one of the most common starting point when mathematically considering insulin-glucose dynamics in vivo, and has been extended, modified and improved by a numerous of scientist worldwide.

Another valuable contribution to the field was the work conducted by Claudio Cobelli and co-workers [60]. In contrast to the fairly uncomplicated nature of the Minimal Model, Cobelli developed a complex, though comprehensive, nonlinear model focusing on modeling the short-term glucoregylatory process in terms of glucose-, insulin- and glucagon dynamics. This was a valuable contribution to the field as the amount of complicated and detailed models were limited.

[8] "In vivo" is a often used medical term with Latin origin meaning "within the living".

In 1985, Salzsieder et al. [61] brought forth a contribution in the diabetes research when he presented an alternative to the short-term glucoregulatory Minimal Model. In the paper "Estimation of individually adapted control parameters for an artificial beta cell" [36], he described the necessity of modeling each diabetic patient individually in order to obtain accurate control parameters in long-term glycemic regulation [36]. The model combined several domains and segments of the glucose-insulin regulation process, e.g. insulin-dependent glucose utilization, insulin catabolism and endogenous glucose production. Through the use of optimal control theory, they were able to optimize the model parameters, and develop a detailed and accurate model, well correlating with medical data and patient information. Jean Pierre Montani and Robert Summers [62, 63] presented a glucose homeostasis model in 1989, focusing on the bi-hormonal glucagon and insulin regulation of glucose [36]. The names Sturis [53], Andreassen [64] and Boroujerdi [65] are also mentioned here as significant contributors to the scientific development within the field of mathematically modeling anatomical control processes.

1.5 Thesis outline

- Chapter 1 - Introduction
  - This chapter will provide the reader a brief introduction to the anatomy related to glucose-insulin control, as well as a historical review of the development within biochemical modeling.
  - It will present segments of the theoretical research conducted.
- Chapter 2 - Enzyme kinetics and biochemical modeling
  - This chapter will present the theory related to glucoregulatory modeling in detail.
- Chapter 3 - Models of the glucoregulatory system
  - In this chapter, the differential equations, model structure and model parameters of all six models will be presented.
- Chapter 4 - Implementation and result
  - This chapter will briefly describe how the models are implemented and simulated in Matlab and Simulink.

  - In will further present and discuss the simulation result of all six models.
  - Based on the simulation results, a modified model will be presented.

- Chapter 5 - Discussion and conclusion
  - Chapter five will present a conclusion of the model study conducted. It will discuss potential sources of errors and possible improvements.
  - Further work will also be suggested in chapter 5.

- Chapter 6 - Appendix
  - Chapter six will present additional material including some of the Matlab and Simulink implementation.
  - An extended portion of additional material in will be attached in the CD.

Chapter 2

Enzyme kinetics and biochemical modeling

This chapter will present how substances in biochemical reaction react and interact. It will also provide a theoretical introduction to biochemical modeling.

2.1 Biochemical reactions and enzyme kinetics

Reactions of the central metabolic pathways are essential for the maintenance of life [19]. Many of these reactions happen spontaneously, while others need *catalyst* for them to happen naturally due to their high energy demand. Catalyst lower the amount of energy needed for the reaction to proceed [19]. Equation 2.1 shows how the enzyme E reacts with the substrate S creating the enzyme-substrate complex ES. Examples of a substrate included in the blood sugar regulatory process is glucose, and the enzymes E might be the hormones insulin and glucagon. The end result is the formation of product P, in our case glycogen or glucose, and the enzyme returns to its initial state, available for reuse. The parameters k_1 and k_{-1} denotes the reaction rate of the forward and reverse reaction of the enzyme-substrate complex respectively, and k_2 is the reaction rate of dissociation of the end product P. In addition to these parameters, we also consider the flow per time unit - the flux 'J'.

$$E + S \underset{k_{-1}}{\overset{k_1}{\rightleftharpoons}} ES \xrightarrow{k_2} E + P \tag{2.1}$$

The way substances in biochemical reaction evolves over time is often described through the use of differential equation on the form represented in equation 2.2 [29].

$$\frac{dx_i}{dt} = synthesis - degradation \pm shuttling... \tag{2.2}$$

$$... \pm complex\ formation \pm chemical\ modification$$

In eq. 2.2, negative signs are associated with a loss-rate, and positive signs with gain-rates. It is the relationship between these rates that describes the dynamics of variable x_i. The steady state level, i.e. $\frac{dx_i}{dt} = 0$, is obtained when the loss-rates equals the gain-rates. A *system* of variables is at steady state when all variables included in the system are at equilibrium.

When considering the glucoregulatory system, we consider a *set* of variables and differential equations. These differential equations and their variables are dependent of one another, meaning that the differential equation describing the dynamics of one variable is a function of the other variables:

$$\frac{dx_i}{dt} = f(x_1, x_2, x_3...x_n)$$

As a tool of solving these differential equations numerically, the software package Matlab has been used.

A central point when considering dynamics is the *order* of biochemical reactions. The order of the reaction describes to what degree the reaction rate is dependent of, or influenced by the concentration of the substances present or active in the reaction. We consider the end-reaction in 2.1 where the enzyme-substrate complex ES form the product P, see equation 2.3.

$$ES \xrightarrow{k_2} E + P \tag{2.3}$$

The dynamics of, or change in the ES-concentration can be described by the law of mass action[1] [18] as follows:

$$\frac{dES}{dt} = -k_2 \cdot E^{\alpha} \cdot S^{\beta} \tag{2.4}$$

The differential equations above describe the dynamics in the concentration of the enzyme-substrate complex ES, while k denotes the reaction rate. The

[1]"The rate of a reaction is proportional to the concentration of the participating molecules" [29].

sum of the indexes α and β determine the order of the reaction. The reaction order is central when considering the substance flow or *flux* 'J' as will be described below.

A zero-order reaction has a reaction rate independent of the concentration of the substance. The reaction rate is therefore constant and unaffected by concentration in E or S. An example of a zero-order reaction is the elimination of blood alcohol which lies on a constant level of 15 milligrams percent per hour ($\pm$5 mg%/hr) regardless of the blood alcohol level [21]. For zero-order reactions, the flux is equal to the reaction rate, see eq. 2.5 [18].

$$J = k \tag{2.5}$$

Where $\alpha = 0$ and $\beta = 0$. If an reaction is of first- or second-order, the reaction velocity is linked to, or dependent on the concentration of substances present in the reaction, i.e. E or S. First-order reaction-fluxes has a linear relation to the substance-concentration as showed in equations 2.6 and 2.7.

$$J = E \cdot k \tag{2.6}$$

$$J = S \cdot k \tag{2.7}$$

Where $\alpha = 1$ or $\beta = 1$. For second-order reactions, the reaction rate k relates to the concentration of E or S in the power of two as follows:

$$J = S^2 \cdot k \tag{2.8}$$

$$J = E^2 \cdot k \tag{2.9}$$

$$J = S \cdot E \cdot k \tag{2.10}$$

Where either $\alpha = 2$ or $\beta = 2$, or both $\alpha = 1$ and $\beta = 1$. Considering a first order reaction where the enzyme E increases the concentration of the substrate S. Keeping the enzyme-concentration at a constant level, the concentration of the substrate will increase. Proportional to this increase, the reaction velocity V will increase in a hyperbolic matter, until it reaches a upper limit, namely V_{MAX}. When the maximum reaction rate is reached, an increase in the substrate-concentration will not influence the reaction rate. This because the enzyme molecules are used to bind substrates, and are unable to accelerate the reaction beyond this point [18]. V_{max} is calculated on the basis of initial enzyme concentration E_0 and catalyst reaction velocity k_{cat}, cf. 2.11.

$$V_{MAX} = k_{cat} \cdot E_0 \tag{2.11}$$

The maximum reaction velocity is also central in the Michelis-Menten equation resented in section 2.2.

2.2 Michaelis-Menten equation

The stating point when considering Michaelis-Menten enzyme kinetics is the curve illustrating the relationship between reaction velocity v_0 and the substrate concentration $[S]$:

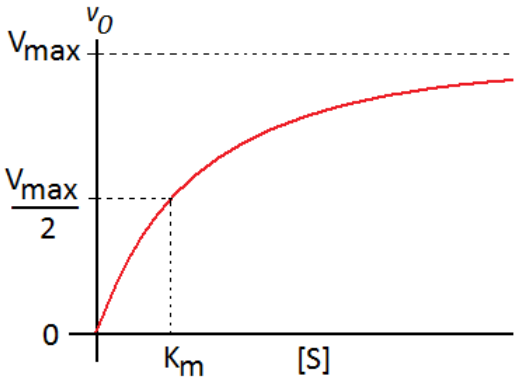

Figure 2.1: Maximum reaction velocity Vmax [19].

Figure 2.1 illustrates the course of the reaction velocity v_0 at increasing substrate concentration $[S]$ [19]. This relationship can be expressed by the Michaelis-Menten equation as follows [19]:

$$v_0 = \frac{V_{max}[S]}{K_m + [S]}$$

Where v_0 is the reaction rate, $[S]$ is the concentration of substrate S, and K_m is the Michaelis-Menten constants defined as follows [19]:

$$K_m = \frac{V_{max}}{2}$$

Considering enzyme kinetics, the Michaelis-Menten equation can be applied as an approximation to describe zero-order enzymatic reactions. As figure 2.1 illustrates, the relationship between the reaction rate v_0, and the substrate concentration $[S]$ has a rectangular hyperbolic shape [19]. At high substrate

concentration $[S]$, the Michaelis-Menten constant K_m becomes negligible in comparison:

$$\frac{lim}{[S] \to \infty} \frac{V_{max}[S]}{K_m + [S]} = V_{max}$$

$$v_0 = V_{max} \tag{2.12}$$

As eq. 2.12 presents, the reaction rate v_0 is now of zero-order with respect to the substrate concentration S [19].

Considering modeling the glucoregulatory system, zero-order enzyme reactions are valuable as they can possibly ensure steady state glucose homeostasis. Instead of assuming strictly zero-order reactions, the more physiologically valid Michaelis-Menten approximation can be applied. Having presented how substances react, it is also a valid point to consider how they influence eachother *within* the reaction or reaction chains. A central aspect of this is substance activation and inhibition, a subject presented in section 2.3.

2.3 Inhibition

An inhibitor is a molecule that restricts or inhibits the enzyme-activity in a reaction. Inhibitors play a vital role in the glucose-regulatory system, and are also essential in many types of medications. Inhibitors bind reversely to the enzyme, preventing the formation of the enzyme-substrate complex ES, or blocks the end reaction inhibiting the dissociation of the product P related to the previously presented equation 2.1 [19]. We separate between competitive-, uncompetitive- and non-competitive inhibition. Competitive inhibition is the most common form of inhibition [19], see equation 2.13.

$$\begin{array}{ccccccccc} & & & & \overset{k_1}{} & & \overset{k_2}{} & & \\ & E & + & S & \rightleftharpoons & ES & \longrightarrow & E & + & P \\ & + & & & \underset{k_{-1}}{} & & & & \\ & I & & & & & & & \\ K_i & \updownarrow & & & & & & & \\ & EI & & & & & & & \end{array} \tag{2.13}$$

In competitive inhibition, the inhibitor I competes with the substrate S over the enzyme E. The enzyme-inhibitor complex EI is formed, leaving the enzyme unable or challenged to catalyze the overall reaction leading to the production of product P.

The inhibitor can also react directly with the enzyme-substrate complex ES in equation 2.1. This principle is shown in equation 2.14 and is known as *uncompetitive inhibition.*

$$\begin{array}{ccccccccc} & & & & k_1 & & k_2 & & \\ E & + & S & \rightleftharpoons & ES & \longrightarrow & E & + & P \\ & & & & k_{-1} & + & & & \\ & & & & & I & & & \\ & & & & K_i & \updownarrow & & & \\ & & & & & ESI & & & \end{array} \tag{2.14}$$

The third category of inhibition is a combination of the mentioned and is called *non-competitive inhibition.* These inhibitors are able to react to both free enzyme molecules, as well as enzyme-substrate complexes creating EI or ESI respectively.

$$\begin{array}{cccccccccc} & & & & & k_1 & & k_2 & & \\ & E & + & S & \rightleftharpoons & ES & \longrightarrow & E & + & P \\ & + & & & k_{-1} & + & & & & \\ & I & & & & I & & & & \\ K_i & \updownarrow & & & K_i & \updownarrow & & & & \\ & & & & & & & & & \\ & EI & + & S & \rightleftharpoons & ESI & & & & \end{array} \tag{2.15}$$

In this report, we will focus on competitive inhibition.

Having introduced inhibition and principles related to biochemical- and enzymatic reactions, we now want to consider these principles in the control engineering domain. For this, we introduce the topic of *physiological controller motifs* [18].

2.4 Controller motifs

Natural controller motifs illustrate how substances in biochemical regulatory processes behave and interact [24]. These controllers present the interaction, activation and inhibition of substances in biochemical reactions and -processes. Depending on how the substances influence each other, natural controllers are classified as either inflow- or outflow controllers [18]. An overview of negative feedback inflow-/outflow controllers are presented in figure 2.2.

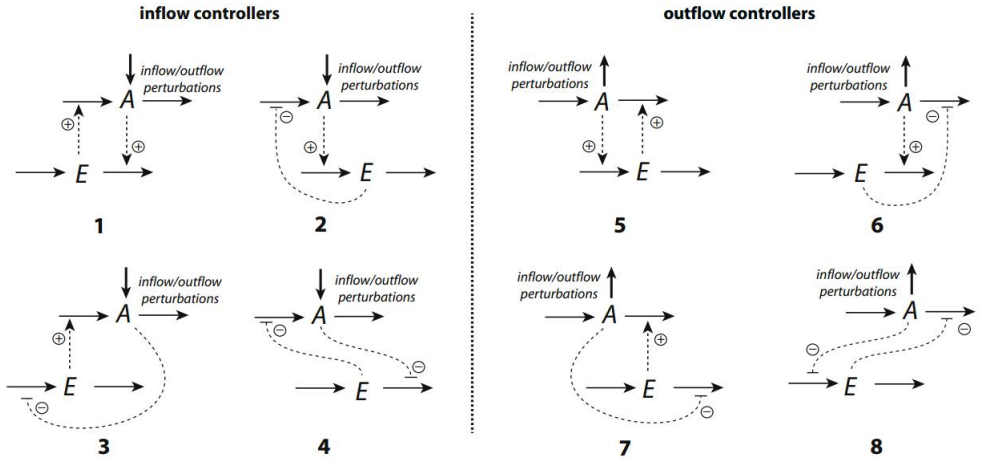

Figure 2.2: Negative feedback inflow-/outflow controllers [18].

Figure 2.2 presents eight structures of two-component homeostatic controller motifs [24]. The substance A is generally considered to be a process, while E is the controller responsible for maintaining homeostasis in process A.

As an example, consider the inflow controller structure 2 in figure 2.2. In this case, the substrate A activates the inflow of the enzyme E, while E has an inhibiting effect on the inflow of substrate A. The practical interpretation of this is that the more the concentration of substrate A increases, the more the inflow in enzyme E will be activated by A. As a result of this activation, the concentration of E will trigger an inhibition of the inflow signal of A, resulting in a reduction of concentration of substrate A.

To relate these principles to the glucoregulatory system, an presentation of the inhibiting and activating relation between substances included in this process is presented below:

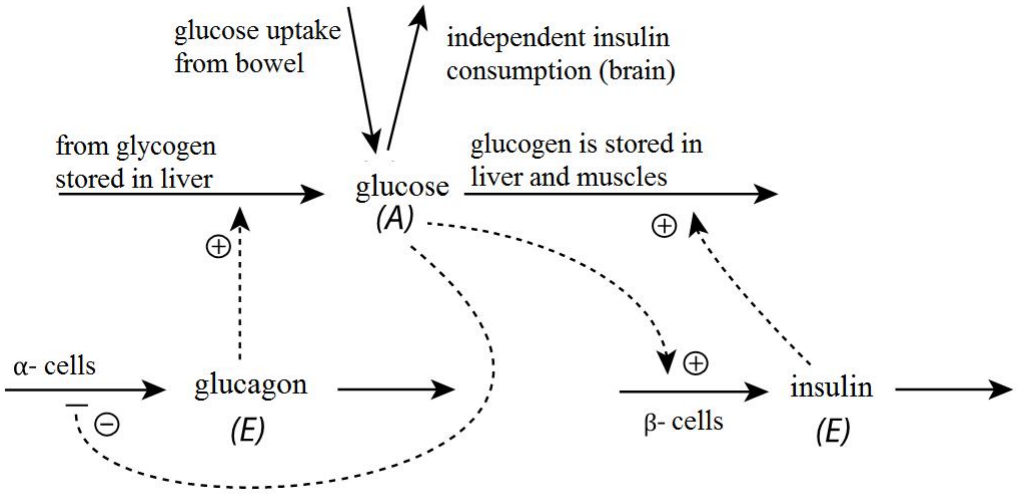

Figure 2.3: Controller motifs in the glucoregulatory system [8].

Figure 2.3 show how the generic substances in the glucose-insulin regulatory system may interact. The main goal of the controllers glucagon and insulin is to maintain homeostasis in process A - plasma glucose concentration. Glucose is taken up from the bowel resulting in an increase of the glucose concentration A. This increase will inhibit the pancreatic α-cells from secreting glucagon, which in turn will mitigate the glucogen decomposition in the liver. Figure 2.3 also illustrates how an increase in A will activate the β-cells causing he insulin concentration to rise. Insulin will then activate the outflow of A in that glucogen is stored in liver and muscle tissue.

Figure 2.3 illustrate the principle of glucose control in a compact and systematic matter. Such a schematic presentation is therefor also used when presenting the respective glucoregulatory models in chapter 3.

2.5 Modeling homeostatic control

A physiologically plausible model is able to simulate homeostatic glucose control. A hypothesis presented by my thesis advisor Tormod Drengstig states that homeostatic control might be related to zero-order degradation. Consider the following example:

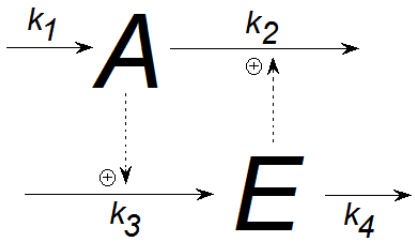

Figure 2.4: Zero order degradation controller motifs.

Figure 2.4 illustrate two substances A and E with their corresponding input-output rates. Based on figure 2.4, the dynamics in A and E can be expressed as follows:

$$\frac{dA(t)}{dt} = k_1 - A(t)E(t) \cdot k_2 \tag{2.16}$$

$$\frac{dE(t)}{dt} = k_3 \cdot A(t) - k_4 \tag{2.17}$$

Based on eq. 2.17, the following steady state expression of $A(t)$ is derived:

$$\frac{dE(t)}{dt} = k_3 \cdot A(t) - k_4 = 0 \tag{2.18}$$

$$k_3 \cdot A(t) = k_4 \tag{2.19}$$

$$A(t) = \frac{k_4}{k_3} \tag{2.20}$$

Expression 2.20 illustrate how zero-order degradation might ensure a controlled $A(t)$ concentration at steady state. To assume zero-order degradation is however a rather physiological unrealistic assumption. The more anatomically valid Michaelis-Menten kinetics is therefor used as a approximation to zero-order degradation. Michaelis-Menten degradation kinetics is introduced in expression 2.21:

$$\frac{dE(t)}{dt} = k_3 \cdot A(t) - k_4 \frac{E(t)}{K_m + E(t)} = 0 \quad where\, K_M \ll E(t)$$

$$A(t) = \frac{k_4}{k_3} \tag{2.21}$$

Equation 2.21 illustrate how $A(t)$ is controlled when Michaelis-Menten kinetics is assumed in the degradation of $E(t)$.

In addition to zero-order degradation and Michaelis-Menten approximation, *auto catalysis* of $E(t)$ might ensures a steady state homeostatic control in $A(t)$, see figure 2.5.

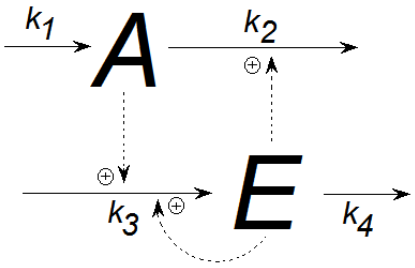

Figure 2.5: Auto catalyzed controller motifs.

Based on figure 2.5, the dynamics of $A(t)$ and $E(t)$ is described as follows:

$$\frac{dA(t)}{dt} = k_1 - A(t)E(t) \cdot k_2$$

$$\frac{dE(t)}{dt} = A(t)E(t) \cdot k_3 - E(t) \cdot k_4$$

The steady state property in $A(t)$ then becomes:

$$\frac{dE(t)}{dt} = A(t)E(t) \cdot k_3 - E(t) \cdot k_4 = 0$$

$$A(t)E(t) \cdot k_3 = E(t) \cdot k_4$$

$$A(t) = \frac{k_4}{k_3}$$

The concentration in $A(t)$ is then stabilized at a steady state level of k_4/k_3. A mathematical model with zero-order degradation, Michaelis-Menten approximation or auto catalysis will therefor supposedly be able to simulate homeostatic integral control.

2.6 Model classification

Glucoregulatory models are often classified as *empirical, semi-empirical* or *physiologically-based* models. Empirical models are developed based on the relationship between a systems input/output data, not focusing on the details within the system itself. These models are valuable when it comes to describe the overall system principle in a simple uncomplicated matter [38].

Semi-empirical models are somewhat more complicated than strictly empirical models. "The goal in such models is to capture the major physiological interactions in order to reproduce the data without sacrificing the structural simplicity" [39]. The system dynamics is captured making these models more versatile, descriptive and extensible than strictly empirical models.

For a more detailed insight of the system, physiologically based models are applied. Related to modeling the insulin-glucose dynamics, a physiologically based model process the metabolic substrates at the intracellular organ/tissue level. These models are time consuming to develop and are made up of a numerous high order- nonlinear differential equations.

The models presented in this chapter are a variety of the three model types mentioned above.

2.7 Model development

Models of the glucoregulatory system are often based on data obtained by one of the two tests: oral glucose tolerance test (OGTT), or intravenous glucose tolerance test (IVGTT). These types of tests are also central in the diabetes diagnostic process.

When conducting an oral glucose tolerance test, a subjects insulin- and glucose levels are measured after eight hours of fasting. Then, the subject orally consumes a certain amount[2] of glucose and the insulin-/glucose levels are remeasured in a three-hour course. Typical result of a OGTT is showed in figure 2.6.

[2]The typical glucose amount is approximately 75 g. [40]

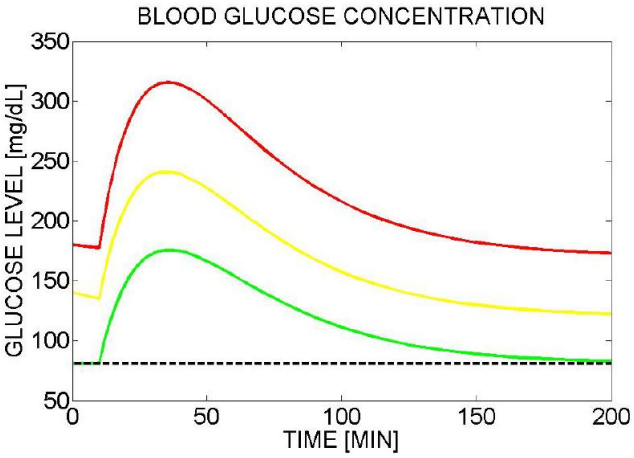

Figure 2.6: The typical result of an oral glucose test showing a normal (green, glucose level $<$ 140 mg/dl), pre-diabetic (yellow, glucose level 140-200 mg/dl), and diabetic response (red, glucose $>$ 200 mg/dl). [40]

Figure 2.6 illustrates the glucose cycle after a oral glucose intake for a normal, pre-diabetic and diabetic subject. The glucose level for healthy subjects (green curve) will rise as a reaction to the glucose intake, but is eventually controlled down to the normal steady state plasma glucose level. The glucose level for non-health subjects (yellow and red curve) will have an initially higher glucose plasma concentration relative to healthy subjects. As figure 2.6 illustrates, the diabetic or pre-diabetic subjects are unable to control the glucose level adequately, hence it is stabilized at a generally higher level.

The same way as the OGTT, an intravenous glucose tolerance test (IVGTT) is able to map a subjects glucose response and -regulation. In addition, IVGTT is used to estimate glucose effectiveness, insulin sensitivity as well as pancreatic responsiveness parameters [40]. The test in itself is carried out though intravenous glucose injections, 0.30g/1kg body weight. The glucose level in the bloodstream is then measured for a three hour period. Typical result of a IVGTT is viewed in figure 2.7.

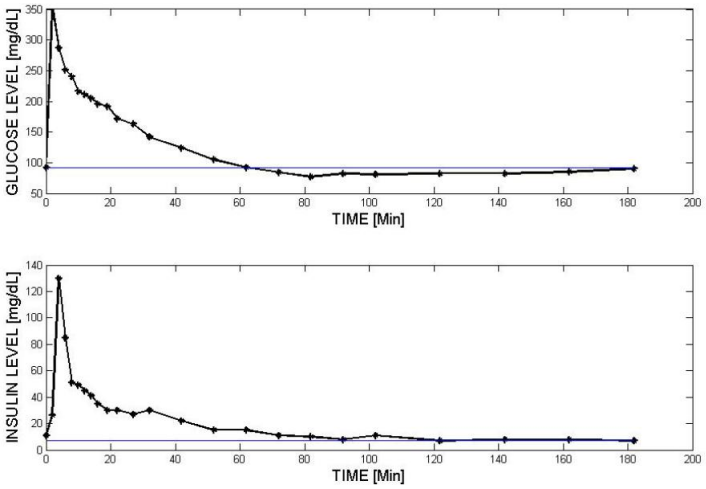

Figure 2.7: The result of an intravenious glucose tolerance test of a healthy subject. [40]

Figure 2.7 illustrates the insulin secretion response to an elevated plasma glucose concentration. The insulin secretion peaks shortly after the detected glucose level elevation, enabling a glucose uptake in muscle and adipose tissue. As a result, the plasma glucose level is lowered. The result of an IVGTT provide valid information regarding mathematical modeling and medical diagnostics.

When comparing the two test forms, the glucose concentrations curve of an IVGTT would have generally steeper slope regarding the initial glucose elevation. This because the glucose is infused directly into the blood stream. As the glucose is infused orally in an OGTT, the glucose elevation would be smoother.

Chapter 3

Models of the glucoregulatory system

This chapter will introduce the glucoregulatory models. The structure, differential equations and model parameters of each model will be presented.

3.1 Choice of models

There are many mathematical models describing glucose regulation. In this thesis, some of the most frequently cited ones are chosen. Individual differences in terms of assumptions, state variables and model structure are studied. The models examined are presented in table 3.1. A short review of the models and how they are linked is presented in the following bullet points.

- The BMM is a empirical minimal model. It is one of the most frequently cited glucoregulatory models.
- The βIG-model is a empirical minimal model. It is developed based on the principles of the BMM, including the dynamics of β-cell mass.
- The βIGIR-model is a modification of the βIG-model. It is an empirical model including the dynamics of insulin receptors.
- The GIE-model is a semi-empirical model. Apart form the GIM-model, it is the most complex of the ones examined. It includes the dynamics of the regulatory hormone glucagon.
- The S&H-model is a minimal empirical model. It is the simplest of the ones examined considering mathematical complexity.

- The GIM-model is the most complex of all the models studied. It is a physiologically-based model with a high level of mathematical complexity. The model is based in a graphic user interface which makes it easily applicable despite its complex model structure.

Model name	**Abbreviation**	**Developed by**	**State variables**
The Bergman Minimal Model (1979)	BMM	Richard N. Bergman [49]	Glucose, insulin and remote insulin
The Glucose-Insulin model (2007)	The GIM-model	Cobelli, Dalla Man, Raimondo and Rizza [30]	Glucose and insulin
The β-cell mass, Insulin and Glucose model (2000)	The βIG-model	Topp, Promislow, Vires, Miura and Finegood [42]	Glucose, insulin and β-cell mass
The β-cell mass, Insulin, Glucose and Insulin Receptor model (2001)	The βIGIR-model	Hernandez, Lyles, Rubin, Voden and Wirkus [43]	Glucose, insulin, β-cell mass and insulin receptors
The Glucose, Insulin and Glucagon model (2006)	The GIE-model	Sulston, Ireland and Praught [36]	Glucose, insulin and glucagon
The Stolwijk and Hardy model (1974)	The S&H-model	Stolwijk and Hardy [44]	Glucose and insulin

Tabell 3.1: Models of the glucoregulatory system.

Having briefly introduced the models, they will now be presented individually in detail. All models have are presented as they are described in their respective articles. The only new thing introduced is the glucose input variable $G_{inn}(t)$, allowing the user to define a glucose input signal common for each model. In chapter 4, two different input signal are applied, one to study the glucose/insulin response to three meals, and another to examine the homeostatic glucose control properties of the models.

3.2 The BMM

Article [49] presents the original Bergman Minimal model. Model parameters, -values and -syntax presented in article [41] is used as supporting material in the presentation and evaluation of the BMM.

When considering the human body as a regulatory system, detailed and complex mathematical models are required to describe this system *accurately*. However, in many cases the aim when modeling is to describe the overall principle in a clear and uncomplicated matter, including only a limited, and necessary amount of detail. Models consisting of a minimal set of equations and parameters, focusing only on describing the system adequately rather than accurately, with a low-as-possible level of complexity can be referred to as *minimal models*. In 1980, Richard N. Bergman, in collaboration with Bowdon, Toffolo and Cobelli, published his minimal model in the paper "Minimal modeling, partition analysis and identification of glucose disposal in animals and man" [40]. The Bergman minimal model is one of the earliest introduced and best known models of the insulin-glucose metabolism in man. Modifications and further development of the Bergman minimal model has contributed to an increased understanding of the human glucoregulatory system. The overall model structure is presented in figure 3.1. The arrows marked in red are used to clarify some of the points presented in the model description.

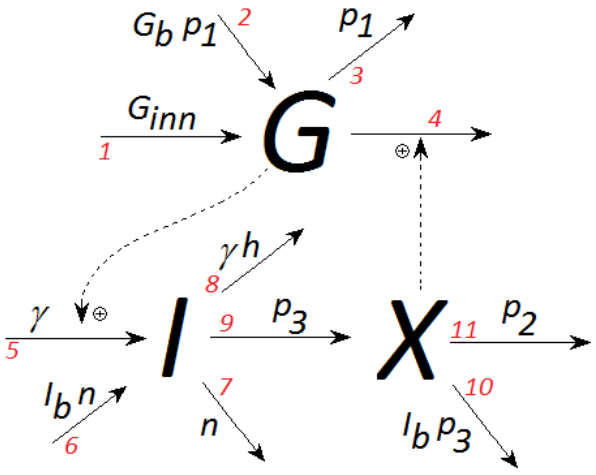

Figure 3.1: Model structure of the BMM.

The model deviation describing the dynamics of each of the state variables; glucose $G(t)$, remote insulin $X(t)$ and insulin $I(t)$ will be presented in the following.

3.2.1 Glucose dynamics

To mathematically describe the glucose dynamics, the mass balance is applied. The description is presented in expression 3.1, and is equal for all the models examined.

$$\frac{dG(t)}{dt} = activation - consumption \tag{3.1}$$

Considering figure 3.1 arrow 1 and 2, the glucose is activated by a basal glucose infusion G_b at rate p_1, and a glucose input signal G_{inn}. The basal glucose infusion G_b is presumably related to the hepatic glucose release. Whereas the input signal G_{inn} is probably related to glucose uptake from food. The activation flux, j_{act} can then be expressed as follows:

$$j_{act} = G_{inn} + G_b p_1 \tag{3.2}$$

The glucose dynamics description has two consumption terms, arrow 3 and 4 figure 3.1. Insulin independent glucose consumption in the brain at rate p_1, and a insulin activated glucose consumption. The latter is most likely describing glucose uptake in muscle- and fat tissue, and in the liver. The glucose consumption flux j_{con} then becomes:

$$j_{con} = p_1 G(t) + X(t)G(t) \tag{3.3}$$

Combining expression 3.2 and 3.3, the complete glucose dynamics becomes the following [41]:

$$\frac{dG(t)}{dt} = G_{inn} - p_1 \left(G(t) - G_b\right) - X(t)G(t) \tag{3.4}$$

3.2.2 Insulin dynamics

To mathematically describe the insulin dynamics, the mass balance is applied. The description is presented in expression 3.5, and is equal for all the models examined.

$$\frac{dI(t)}{dt} = activation - degradation \tag{3.5}$$

An increase in the insulin concentration is activated by two term in the BMM, arrow 5 and 6 figure 3.1. A increased glucose concentration activates the insulin secretion with a rate γ. In addition, the insulin dynamic has a basal secretion I_b at rate n. The insulin activation flux is then expressed as follows:

$$j_{act} = I_b n + \gamma G(t) \tag{3.6}$$

The insulin concentration has two degradation terms, arrow 7 and 8 figure 3.1. One first order term associated with the degradation rate n, and a zero-order degradation. This zero-order degradation is interesting in terms of homeostatic control and will be examined further in chapter 4. The complete insulin degradation flux j_{deg} is expressed as follows:

$$j_{deg} = nI(t) + \gamma h \tag{3.7}$$

Expression 3.6 and 3.7 is combined resulting in the complete insulin dynamics description [41]:

$$\frac{dI(t)}{dt} = -n\left(I(t) - I_b\right) + \gamma\left(G(t) - h\right))$$

3.2.3 Remote insulin in action

In addition to glucose and insulin, the BMM describes the insulin effect on the net glucose disappearance, or remote insulin in action $X(t)$ [41]. Figure 3.1, arrow 9 illustrate how the insulin concentration $I(t)$ activates the remote insulin $X(t)$, which in turn activates the glucose degradation. Remote insulin is has a first- and zero-order degradation, arrow 11 and 10 respectively. The zero-order degradation term will be further discussed in chapter 4. The complete expression of the remote insulin dynamics becomes [41]:

$$\frac{dX(t)}{dt} = -p_2 X(t) + p_3\left(I(t) - I_b\right) \tag{3.8}$$

3.2.4 Complete model

The BMM as a whole is presented in eq. 3.9, 3.10 and 3.11 [41]. Model parameters are presented in table 3.2.

$$\frac{dG(t)}{dt} = G_{inn} - p_1\left(G(t) - G_b\right) - X(t)G(t) \tag{3.9}$$

$$\frac{dX(t)}{dt} = -p_2 X(t) + p_3\left(I(t) - I_b\right) \tag{3.10}$$

$$\frac{dI(t)}{dt} = -n\left(I(t) - I_b\right) + \gamma\left(G(t) - h\right) \tag{3.11}$$

Parameter	**Value**	**Description**	**Unit**
$G(t)$		Plasma glucose concentration	mg/dl
$I(t)$		Plasma insulin concentration	µU/ml
$X(t)$		Remote insulin action	min^{-1}
G_b	60.0	Basal injection level of glucose	mg/dl
I_b	7.0	Basal injection of insulin	µU/ml
p_1	0.03	Insulin-independent rate constant of glucose uptake in muscle, liver and adipose tissue	min^{-1}
p_2	0.01	Rate for decrease in tissue glucose uptake ability	min^{-1}
p_3	0.00001	Insulin-dependent increase in glucose uptake ability in tissue per unit of insuin consentration above I_b	min^{-2} $(\mu U/ml)^{-1}$
n	0.3	First order decay rate for insulin in plasma	min^{-1}
h	17.04	Threshold value for glucose, above which the pancreatic β-cells release insulin	mg/dl
γ	0.004	Rate of the insulin release after the glucose injection and with glucose consentration above h	$\frac{\mu U}{ml}\, min^{-2}$ $(mg/dl)^{-1}$
G_0	60.0	Initial glucose concentration	mg/dl
I_0	7.0	Initial insulin concentration	µU/ml
X_0	0	Initial remote insulin concentration	min^{-1}

Tabell 3.2: Model parameters of the Bergman minimal model [41].

3.3 The βIG-model

This model was developed by Brian Topp et al. and was presented in the Journal of Theoretical Biology in 2000 [42]. The model describes the dynamics of glucose, insulin and β-cell mass in the glucoregulatory process. The dynamics of the β-cell mass was included in the model inspired by studies conducted by Leahy (1990) and Tobin et al. (1992) [42]. The point is to study the homeostatic properties with limited β-cell functionality, assuming normal insulin sensitivity. A schematic of the model is presented in figure 3.2. The arrows are indexed with red numbers to clarify some points in the model description.

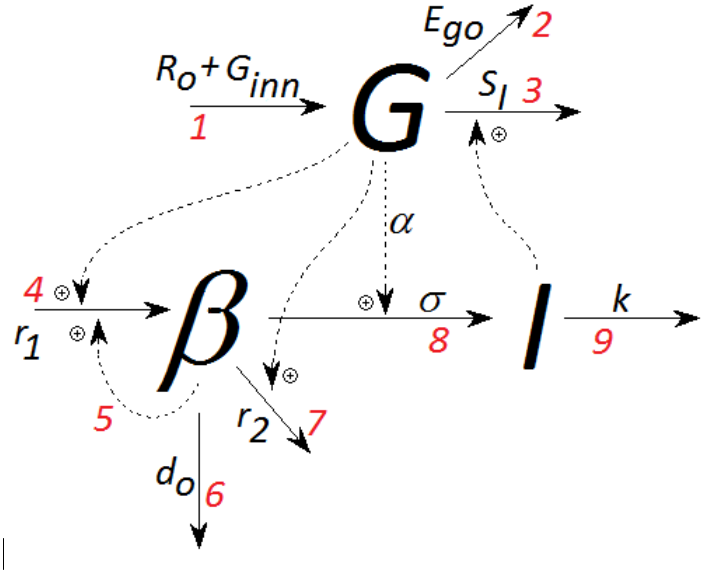

Figure 3.2: The model schematics of the βIG- model.

The model deviation describing the dynamics of each of the state variables; glucose $G(t)$, insulin $I(t)$ and β-cell mass $\beta(t)$ will be presented in the following.

3.3.1 Glucose dynamics

Figure 3.2 arrow 1 illustrate the glucose activation. It has a basal level R_0, and a glucose input signal associated with food intake G_{inn}. The activation flux is expressed as follows:

$$j_{act} = G_{inn} + R_0$$

The glucose is consumed independent from the insulin concentration by the brain at a rate E_{go}, arrow 2 figure 3.2. The glucose uptake has also a first order term, cf. figure 3.2 arrow 3. This flux describes how the peripheral glucose uptake, at rate S_I, is accelerated by an elevated insulin concentration [42]. The total glucose consumption then becomes:

$$j_{con} = G(t)E_{go} + S_I \cdot I(t)G(t)$$

Combining the activation- and consumption flux, the complete description of the glucose dynamics is expressed as follows [42]:

$$\frac{dG(t)}{dt} = G_{inn} + R_0 - (E_{go} + S_I \cdot I(t))\, G(t)$$

3.3.2 Insulin dynamics

Insulin $I(t)$ is activated by a elevation in the glucose concentration $G(t)$. Insulin is also activated by the β-cell mass $\beta(t)$, as the β-cells secrete insulin. The parameter σ denotes the maximum β-cell insulin secretion rate. The model describes this insulin activation, arrow 8 figure 3.2, as a sigmodial function of the plasma glucose concentration $G(t)$ with an associated function parameter α. This consideration is adopted form studies conducted by Cobelli et al. (1980) and Rudenski et al. (1991). The sigmodial activation flux is is expressed as follows:

$$j_{act} = \beta(t)\sigma\frac{G(t)^2}{G(t)^2 + \alpha}$$

The parameter k is related to the combined first order insulin degradation in liver, kidneys and insulin receptors. It is indicated as arrow 9 in figure 3.2, and expressed as follows:

$$j_{deg} = I(t)k$$

The activation- and degradation flux is combined to form the complete insulin dynamics expression [42]:

$$\frac{dI(t)}{dt} = \frac{\beta(t)\sigma G(t)^2}{G(t)^2 + \alpha} - kI(t) \tag{3.12}$$

3.3.3 β-cell mass dynamics

The dynamics of the β-cell mass is included in this glucoregulatory model to how normal glucose control can be maintained in spite of limited β-cell functionality, assuming normal insulin sensitivity [42]. The βIG-model assumes slow process dynamics related to the β-cell mass. This is the reason for the time scale being in days and not hours or minutes [42]. The mass balance provides the following expression of the β-cell mass dynamics:

$$\frac{d\beta(t)}{dt} = synthesis - degradation$$

The β-cell synthesis is activated by an elevation in the glucose concentration $G(t)$. In addition, the synthesis is auto catalyzed by the β-cell mass it self $\beta(t)$. A hypothesis presented by my thesis advisor suggest that such a auto catalysis can ensure steady state homeostatic control. Homeostatic model property is a central focus point is this thesis and will therefore be further discussed in chapter 4. The synthesis is associated with a rate constant r_1 and is expressed as follows:

$$j_{syn} = r_1 G(t)\beta(t)$$

The degradation of the β-cell mass is modeled in two terms. One first order term associated with the natural death of β-cells with rate constant d_0, cf. arrow 6 figure 3.2. The limitation in β-cell functionality is modeled as a three order term activated by the glucose concentration $G(t)$. This β-cell degradation is associated with the rate constant r_2 and illustrated as arrow 7 in figure 3.2. The complete β-cell mass degradation flux becomes the following:

$$j_{deg} = d_0\beta(t) + r_2 G(t)^2\beta(t)$$

The synthesis and degradation expression is then combined to form the complete description of the β-cell mass dynamics [42]:

$$\frac{d\beta(t)}{dt} = \left(-d_0 + r_1 G(t) - r_2 G(t)^2\right)\beta(t)$$

3.3.4 Complete model

The βIG-model as a whole is presented in eq. 3.13, 3.14 and 3.15 [42]. The model parameters are presented in table 3.3

$$\frac{dG(t)}{dt} = G_{inn} + R_0 - (E_{go} + S_I I(t))\, G(t) \tag{3.13}$$

$$\frac{dI(t)}{dt} = \frac{\beta(t)\sigma G(t)^2}{G(t)^2 + \alpha} - kI(t) \tag{3.14}$$

$$\frac{d\beta(t)}{dt} = \left(-d_0 + r_1 G(t) - r_2 G(t)^2\right) \beta(t) \tag{3.15}$$

Parameter	Value	Description	Unit
$G(t)$		Plasma glucose consentration	$mg\, dl^{-1} d^{-1}$
$I(t)$		Plasma insulin consentration	$\mu U ml^{-1}$
$\beta(t)$		Mass of pancreatic β-cells	mg
$\frac{G^2}{\alpha - G^2}$		Hill function, a sigmoid ranging from 0 to 1 reaching half its maximum at $G = \alpha^{0.5}$	
R_0	864	Net rate of production at zero glucose	$mg\, dl^{-1} d^{-1}$
E_{go}	1.4	Glucose effectiveness at zero insulin for production and uptake	d^{-1}
S_I	0.7	Total insulin sensitivity	$\mu U ml^{-1} d^{-1}$
σ	43.2	Maximum β-cell insulin secretion rate	$\mu U ml^{-1} d^{-1}$
k	432.0	Combined insulin uptake at the liver,kidneys and insulin receptors	d^{-1}
α	20,000	Parameter of the Hill function $\frac{G^2}{\alpha - G^2}$	$mg^2 dl^{-2}$
d_0	0.06	The β-cell death rate at zero glucose	d^{-1}
r_1	0.84×10^{-3}	Rate constant	$mg^{-1} dl\, d^{-1}$
r_2	0.24×10^{-5}	Rate constant	$mg^{-2} dl^2 d^{-1}$

Tabell 3.3: Model parameters for The βIG-model [42].

3.4 The βIGIR-model

The βIGIR-model is a modification of the previously described βIG-model, including the dynamics of insulin receptors $R(t)$. The βIG-model describes how normal glucose control can be maintained at reduced β-cell functionality, when normal insulin sensitivity is assumed. Whereas the βIGIR-model describes how normal blood sugar regulation is maintained assuming reduced insulin sensitivity. A lower-than-normal insulin sensitivity has been documented in pubertal, obese and aging subjects and during pregnancy, who are still able to maintain healthy plasma glucose control [43]. The model structure is presented in figure 3.3.

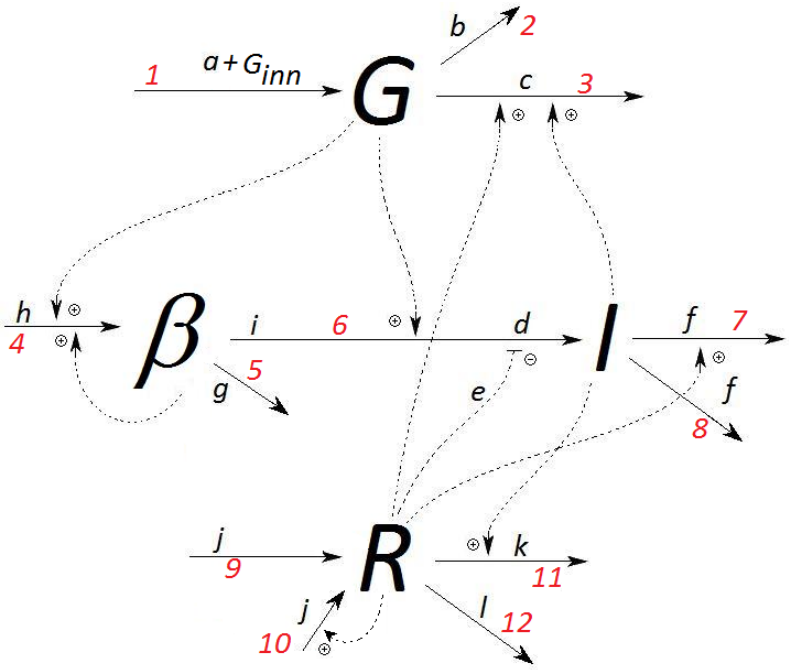

Figure 3.3: Structural overview of the βIGIR-model.

A description of the state variable dynamics is presented in the following.

3.4.1 Glucose dynamics

Equal to the βIG-model, the βIGIR-model has a basal insulin activation with rate constant a, in addition to a glucose input signal related to food intake G_{inn}. The glucose activation flux is indexed 1 in figure 3.3 and is expressed as follows:

$$j_{act} = a + G_{inn}$$

The glucose consumption by the brain is independent from both insulin $I(t)$, and insulin receptors $R(t)$ [43]. Rate constant b is associated with this consumption and illustrated as flux 2 in figure 3.3. The peripheral glucose consumption with rate constant c , flux 3 in figure 3.3, is activated by both insulin $I(t)$, and insulin receptors $R(t)$. The complete consummation flux becomes:

$$j_{con} = G(t)b + cR(t)I(t)G(t)$$

The activation and consummation flux is combined to form the complete glucose description:

$$\frac{dG(t)}{dt} = G_{inn} + a - (b + cR(t)I(t))\,G(t) \tag{3.16}$$

3.4.2 Insulin dynamics

The insulin activation is described using the same sigmodial function as seen in the βIG-model. In addition, the insulin receptors $R(t)$ affect the insulin activation. The insulin receptors is a number from 0-1, where 0 indicate 100% insulin resistance. Hence, a healthy person would have a $R(t)$ value close to 1. A person with limited insulin sensitivity needs a higher plasma insulin concentration to maintain glucose control. This is modeled as follows:

$$j_{act} = \frac{d\beta(t)G(t)^2}{e + G(t)^2} \cdot \frac{1}{1 + R(t)}$$

The degradation is described using two terms indexed 7 and 8 in figure 3.3. Flux 8 is of first order in respect to the insulin concentration $I(t)$, and flux 7 is activated by the fraction of insulin receptors $R(t)$. The rate constant f is related to both terms. The degradation flux becomes:

$$j_{deg} = fI(t) + fR(t)I(t)$$

The activation and degradation flux is combined to form the complete insulin dynamics description:

$$\frac{dI(t)}{dt} = \frac{d\beta(t)G(t)^2}{(1+R(t))\,(e+G(t)^2)} - fI(t) - fR(t)I(t) \tag{3.17}$$

The β-cell dynamics is equal to the one described in the βIG-model, and will therefor not be repeated.

3.4.3 The dynamics of insulin receptors

The mass balance provide the following description of the insulin receptor dynamics [43]:

$$\frac{dR(t)}{dt} = recycling - reduction$$

Figure 3.3 indicate two recycling terms, one independent and one dependent from the insulin receptor dynamics $R(t)$. The terms are indexed 9 and 10 respectively and is expressed as follows:

$$j_{rec} = j + jR(t)$$

The reduction in insulin receptors is primarily the result of endocyntosis [43]. Endocyntosis is the process of molecules being absorbed by cells. Figure 3.3 illustrate a insulin dependent and insulin independent reduction flux, indexed 11 and 12 respectively. The fluxes with their associated rate constants, k and l respectively is expressed as follows:

$$j_{red} = kI(t)R(t) + lR(t)$$

The insulin receptor dynamics is described as follows [43]:

$$\frac{dR(t)}{dt} = j\,(1+R(t)) - kI(t)R(t) - lR(t) \tag{3.18}$$

3.4.4 Complete model

The βIGIR-model is presented as a whole in equation 3.19-3.22 [43]. Model parameters are presented in table 3.4

$$\frac{dG(t)}{dt} = a - (b + cR(t)I(t))\,G(t) \tag{3.19}$$

$$\frac{dI(t)}{dt} = \frac{d\beta(t)G(t)^2}{(1+R(t))\,(e+G(t)^2)} - fI(t) - fR(t)I(t) \tag{3.20}$$

$$\frac{d\beta(t)}{dt} = \left(-g + hG(t) - iG(t)^2\right) \cdot \beta \tag{3.21}$$

$$\frac{dR(t)}{dt} = j\left(1 + R(t)\right) - kI(t)R(t) - lR(t) \tag{3.22}$$

Parameter	**Value**	**Description**	**Unit**
a	864	Glucose production rate by liver at zero glucose consentration	mg/dl d
b	1.4	Insulin independent glucose clerance rate	1/d
c	0.9	Insulin induced glucose uptake rate	ml/μU d
d	43.2	Maximum β-cell insulin secretion rate	μU/ml d mg
e	20 000	Gives inflection point of sigmodial function	mg^2/dl^2
f	216	Insulin clerance rate	1/d
g	0.03	β-cell death rate	1/d
h	0.57×10^{-3}	Determines β-cell glucose tolerance rate	dl/mg d
i	0.25×10^{-5}	Determines β-cell glucose tolerance rate	dl^2/mg^2d
j	2.6	Insulin receptors recycling rate	1/d
k	0.020	Insulin dependent receptor endocytosis rate	ml/μU d
l	0.2	Insulin independent receptor endocytosis rate	1/d

Tabell 3.4: Model parameters for the βIGIR-model [43].

3.5 The GIE-model

Studies conducted by Celeste et al. [50] and Summers and co-workers [51, 52] suggests that a weighted combination of insulin and glucagon has an effect on the regulation of the plasma glucose levels [36]. This is the motivation as to why glucagon is included as a state variable, $E(t)$, in the GIE-model. Being a semi-empirical model it has a markedly higher complexity level than the previously mentioned models. The overall model structure is presented in figure 3.4.

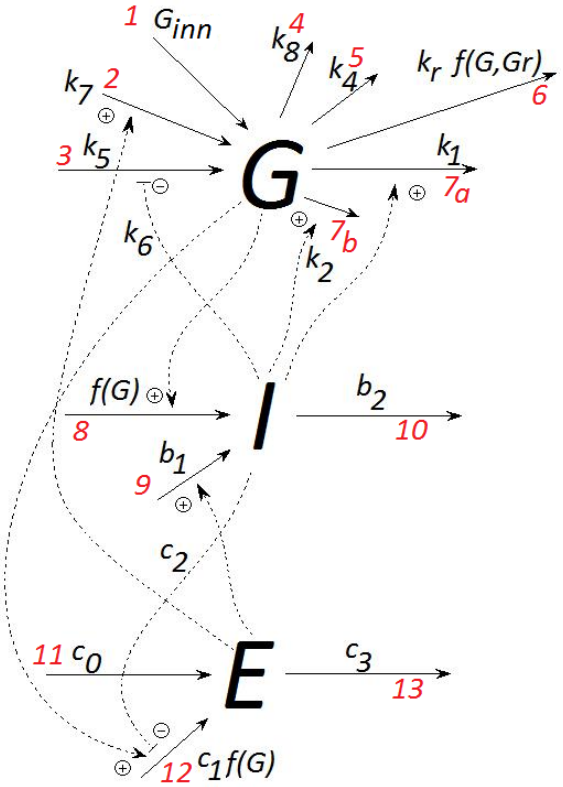

Figure 3.4: Schematic presentation of the GIE-model.

Figure 3.4 illustrate the complexity of the model. To get a systematic overview, the dynamics of each state variable is presented in the following.

3.5.1 Glucose dynamics

The input signal G_{inn} is based on the original input signal of the GIE-model, $G_{exg}(t)$. This signal describes the glucose absorption through food, and is developed by Yates and Fletcher [48]. It is described in detail in appendix B.

Glucose is modeled with three activation terms. One related to food intake, G_{inn} marked 1 in figure 3.4, and two describing hepatic glucose release, indexed 2 and 3. Arrow 2 describes a glucose release from the liver, with associated rate constant k_7, activated by glucagon $E(t)$. Arrow 3 is also related to hepatic glucose release, inhibited by insulin $I(t)$, with associated rate constants k_5 and k_6. The glucose activation flux is expressed as follows:

$$j_{act} = G_{inn} + k_5 \frac{k_6}{k_6 + I(t)} + k_7 E(t) \tag{3.23}$$

A remark considering the activation term $k_7 E(t)$ in eq. 3.23. This term is independent from the glucose concentration $G(t)$. This implyes that glucagon will activate the hepatic glucose release even at high plasma glucose concentration, something that is seemingly unwanted and physiologically unreasonable.

The GIE-model describes glucose to be consumed in four terms, arrow 4-7 figure 3.4. Arrow 5 represents the insulin independent glucose consumption by the brain, at max rate k_4. Insulin dependent glucose consumption in peripherals, with associated rate constants k_1 and k_2, is indexed 7a and 7b. In addition, the GIE-model describes renal glucose uptake when the plasma glucose concentration exceeds the threshold value $G_r = 180$ mg/dl [36]. The renal glucose uptake is controlled using a threshold function, and the rate constant k_r. Glucose is also consumed in the liver. The renal and hepatic glucose consumption is indexed 6 and 4 in figure 3.4 respectively. The complete glucose consumption is expressed as follows:

$$j_{con} = k_8 \frac{G(t)}{k_9 + G(t)} + k_4 \frac{G(t)}{k_3 + G(t)} + (k_1 G(t) + k_2)\, I(t) + k_r\, (G(t) - G_r)\, u\, (G - G_r) \tag{3.24}$$

A remark considering the peripheral uptake $(k_1 G(t) + k_2)\, I(t)$ eq. 3.24. The consummation term $k_2 I(t)$, implies that glucose will be consumed in muscle and fat tissue independent form the glucose concentration. Thus even at low plasma glucose concentration, it will be further reduced by this insulin activated peripheral uptake. This does not seem physiologically plausible and is therefor commented.

The activation and degradation flux is combined forming the complete glucose dynamics description [36]:

$$\frac{dG(t)}{dt} = G_{inn} + \frac{k_5 k_6}{k_6 + I(t)} - \frac{k_8 G(t)}{k_9 + G(t)} + k_7 E(t) - \frac{k_4 G(t)}{k_3 + G(t)} - (k_1 G(t) + k_2)\, I(t)$$

$$-k_r \left(G(t) - G_r\right) u \left(G(t) - G_r\right)$$

3.5.2 Insulin dynamics

The GIE-model describes the insulin dynamics of having two activation terms. On first order term activated by glucagon $E(t)$ with associated rate constant b_1, cf arrow 9 figure 3.4. In addition, insulin is modeled as a hyperbolic tangent function dependent of glucose. This insulin activation model is adopted from Sturis et al. [53]. In addition to the two terms, the model enables the user to specify a exogenous insulin input signal related to diabetic model simulation. As the focus point in this thesis is healthy blood sugar regulation, this term is neglected. The insulin activation flux is described as follows:

$$j_{act} = \frac{a_1}{2} \left[tanh\left(a_2 \left(G(t) - a_3\right)\right) + 1\right] + b_1 E(t)$$

Insulin is modeled with a first order degradation with rate constant b_2:

$$j_{deg} = b_2 I(t)$$

The complete insulin dynamics description becomes [36]:

$$\frac{dI(t)}{dt} = \frac{a_1}{2} \left[tanh\left(a_2 \left(G(t) - a_3\right)\right) + 1\right] + b_1 E(t) - b_2 I(t)$$

3.5.3 Glucagon dynamics

The mass balance is applied to describe the glucagon dynamics:

$$\frac{dE(t)}{dt} = secretion - degradation$$

Figure 3.4 illustrate how the glucagon secretion is described using two terms, marked 11 and 12. Arrow 11 indicate the basal secretion at rate c_0. Secretion 12 is activated by glucose $G(t)$, inhibited by insulin $I(t)$, and is modeled combining the Heavyside step function with the threshold function G_E [36]. When the plasma glucose concentration falls bellow the threshold $G_E = 75$

mg/dl, glucagon is secreted to restore glucose homeostasis. This secretion is inhibited by insulin, as a high insulin concentration implies a high plasma glucose concentration. Glucagon has max secretion rate $\frac{c_1}{c_2}$ at $I(t) = 0$. The secretion flux is presented in equation 3.25.

$$j_{sec} = c_0 + \frac{c_1}{c_2 + I(t)} \left(G_E - G(t)\right) u \left(G_E - G(t)\right) \tag{3.25}$$

Glucagon is modeled with first order degradation with corresponding rate constant c_3:

$$j_{deg} = c_3 E(t)$$

The complete glucagon dynamics becomes the following [36]:

$$\frac{dE(t)}{dt} = c_0 + \frac{c_1}{c_2 + I(t)} \left(G_E - G(t)\right) u \left(G_E - G(t)\right) - c_3 E(t) \tag{3.26}$$

3.5.4 Complete model

The complete GIE-model is presented in eq. 3.27-3.29 [36]. Model parameters are presented in table 3.5 and 3.6.

$$\frac{dG(t)}{dt} = G_{inn} + \frac{k_5 k_6}{k_6 + I(t)} - \frac{k_8 G(t)}{k_9 + G(t)} + k_7 E(t) - \frac{k_4 G(t)}{k_3 + G(t)} \tag{3.27}$$

$$- \left(k_1 G(t) + k_2\right) \cdot I(t) - k_r \left(G(t) - G_r\right) u \left(G(t) - G_r\right)$$

$$\frac{dI(t)}{dt} = \frac{a_1}{2} \left[tanh(a_2(G(t) - a_3)) + 1\right] + b_1 E(t) - b_2 I(t) \tag{3.28}$$

$$\frac{dE(t)}{dt} = c_0 + \frac{c_1}{c_2 + I(t)} \left(G_E - G(t)\right) u \left(G_E - G(t)\right) - c_3 E(t) \tag{3.29}$$

Parameter	Value	Description	Unit
k_1	$1.1{\cdot}10^{-4}$	Insulin dependent glucose uptake rate by peripherals	min^{-1}per (ng/dl of I)
k_2	$9.8{\cdot}10^{-3}$	Insulin dependent glucose uptake rate by peripherals	min^{-1}per (ng/dl of I)
k_3	207.1	Insulin independent glucose uptake rate in brain	mg/dl
k_4	9.1	Insulin independent glucose uptake rate in brain	mg/dl/min
k_5	25.3	Maximum glucose release rate	mg/dl/min
k_6	149.8	"Damping" factor	ng/dl of I
k_7	0.45	Glucagon dependent hepatic glucose release rate	mg/dl/min
k_8	35.4	Glucose saturation parameter	mg/dl/min
k_9	73.0	Glucose saturation parameter	mg/dl
k_r	0.04	Uptake rate control parameter	min^{-1}
G_r	180.0	Renal glucose threshold	mg/dl
T_{asc}	15.0	Duration of the ascending branch of the gastric emptity curve	min
T_{desc}	15.0	Duration of the decending branch of the gastric emptity curve	min
V_{max}	360.0	Maximum rate of gastric emptity	mg/min
K_{gabs}	1/60	Absorption rate constant of glucose from the gut	min^{-1}

Tabell 3.5: Model parameter of the GIE-model [**?**]

Parameter	Value	Description	Unit
a_1	248.8	Maximum secretion rate in the absence of glucagon	ng/dl/min
a_2	0.02	Parameter defining insulin secretion	$(\text{mg/dl})^{-1}$
a_3	198.0	Parameter defining insulin secetion	mg/dl
b_1	0.14	The dependence of insulin on glucagon	(ng/dl/min of I) per (ng/dl of E)
b_2	0.2	Insulin decay constant	min^{-1}
c_0	0.65	Basal glucagon secretion rate	ng/dl/min
c_1	2.5	Glucagon secretion parameter	(ng/dl/min of E) per (mg/dl of G)
c_2	-5.25	Glucagon secretion parameter	ng/dl of I
c_3	0.08	Glucagon degradation	min^{-1}
G_E	75.0	Threshold value	mg/dl

Tabell 3.6: Model parameter of the GIE-model [**?**]

3.6 The S&H-model

When using mathematical models to describe nonlinear complex anatomical processes, simplifications are made. The central point is to make *reasonable* simplifications and assumptions without compromising the clinical validity or -plausibility of the model. The Stowijk and Hardy empirical minimal model describes "Regulation of blood glucose using physiologic data to determine the numeric coefficients and making simplifying assumptions to limit the complexity of the equations." [45]. It is the least complex of all the models examined, comprising only two state variables, namely glucose $G(t)$ and insulin $I(t)$. The model is schematically presented in figure 3.5.

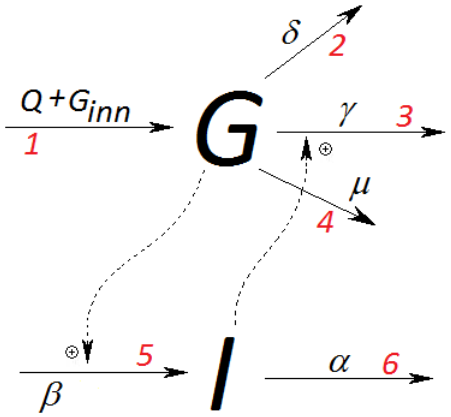

Figur 3.5: Model schematics of the S&H-model.

The dynamics of the glucose- and insulin concentration is presented in the following.

3.6.1 Glucose dynamics

As previously seen, the glucose is activated by a basal glucose infusion in addition to the input signal G_{inn}, highlighted as flux 1 figure 3.5:

$$j_{act} = Q + G_{inn}$$

The glucose degradation is described using three terms. Arrow 2 indicate the insulin independent glucose uptake in the brain, with rate constant δ. Flux 3 represents the insulin dependent glucose uptake in peripheral tissue with corresponding rate constant γ. Common with the GIE-model, the S&H-model also include a renal glucose degradation, indexed 4 in figure 3.5. This

degradation is modeled to occur when the plasma glucose level exceeds the threshold value $G_K = 250$ mg/dl, which is a higher, seemingly more reasonable threshold value than the one used in the GIE-model - $G_r = 180$ mg/dl. The renal glucose degradation is associated with the rate constant μ. The complete degradation flux becomes:

$$j_{deg} = \gamma I(t)\,(G(t) - G_t) + \delta\,(G(t) - G_t) + \mu\,(G(t) - G_K)$$

The parameter G_t denotes the effective intracellular glucose concentration and defined as $G_t = 0$ [36]. Is is therefor neglected in the following. The complete glucose dynamics description then becomes [44]:

$$C_G \frac{dG(t)}{dt} = Q + G_{inn} - \gamma I(t)G(t) - \delta G(t) - \mu\,(G(t) - G_K) \tag{3.30}$$

Where C_G is the volume scaling factor [44]

3.6.2 Insulin dynamics

The S&H-model describes insulin secretion to be activated when the plasma glucose exceeds the threshold level $G_0 = 51.0$. The activation flux is marked 5 in figure 3.5, and is associated with the rate constant β:

$$j_{act} = \beta\,(G(t) - G_0)$$

The insulin degradation flux is of first order in respect to the insulin concentration $I(t)$, with corresponding rate constant α:

$$j_{deg} = \alpha I(t)$$

The complete insulin concentration dynamics is expressed as follows [44]:

$$C_i \frac{dI(t)}{dt} = \beta\,(G(t) - G_0) - \alpha I(t)$$

A remark to the insulin dynamics is that by extending the parenthesis, a zero-order degradation term is obtained:

$$C_i \frac{dI(t)}{dt} = \beta G(t) - \alpha I(t) - \beta G_0$$

This is a interesting dynamics feature considering modeling homeostatic glucose control, and will be further discussed in chapter 4

3.6.3 Complete model

The complete S&H-model is expressed in eq. 3.31 and 3.32 [44]. Model parameters are presented in table 3.7 [44].

$$C_G \frac{dG(t)}{dt} = G_{inn} + Q - \gamma I(t)G(t) - \delta G(t) - \mu(G(t) - G_K) \tag{3.31}$$

$$C_i \frac{dI(t)}{dt} = \beta(G(t) - G_0) - \alpha I(t) \tag{3.32}$$

Parameter	Value	Description	Unit
$G(t)$		Glucose consentraiton of extracellular space	mg%
$I(t)$		Insulin consentraiton of extracellular space	mU%
α	76.0	Coefficient for insulin destruction	$\text{mUhr}^{-1}\cdot\text{mU\%}^{-1}$
β	14.3	Coefficient for insulin secretion	$\text{mUhr}^{-1}\cdot\text{mg\%}^{-1}$
δ	24.7	Coefficient for insulin independent glucose utilization	$\text{mUhr}^{-1}\cdot\text{mg\%}$
γ	13.9	Coefficient for insulin effect on glucose utilization	$\text{mg}\cdot\text{hr}^{-1}\cdot\text{mg\%}^{-1}\cdot\text{mU\%}^{-1}$
μ	72.0	Coefficient for gllucose loss in urine	$\text{mg}\cdot\text{hr}^{-1}\cdot\text{mg\%}^{-1}$
G_t	0.0	Effective intracellular glucose consentration	mg%
G_0	51.0	Threshold consentration of glucose for insulin secretion	mg%
G_K	250.0	Tubular reabsorption maximum for glucose	mg%
C_G	150.0	Glucose capacitance for extra cellular space	$\text{mg}\cdot\text{mg\%}^{-1}$
C_i	150.0	Insulin capacitance for extra cellular space	$\text{mU}\cdot\text{mU\%}^{-1}$
Q	8,400	Basal glucose release into extracellular space	$\text{mg}\cdot\text{hr}^{-1}$

Tabell 3.7: Model parameters on the S&H-model.

3.7 The GIM-model

The glucose-insulin model (GIM) is the most mathematically complex of the ones studied in this thesis. The model is a GUI[1]-based meal simulation software developed by Dalla Man, Raimondo, Riazza and Cobelli [30]. The GUI allows the user to simulate the glucose- and insulin levels of a healthy-, type 1 diabetic- and type 2 diabetic subject, with limited to no modeling competence. The model has been derived based on a data collection from 204 healthy subjects between 54 and 58 years, weighing 77-79 kg, as well as 14 type 2 diabetic subjects from 54 to 60 years, weighing 86-96 kg [31]. The parameters are numerically calculated based on measured concentration and fluxes, minimizing the deviation between the model and measured data values through the use of the nonlinear least squares method. Details regarding the model structure will not be presented as the simulation is based on the graphical user interface. This will illustrate how applicable the model is in spite of its high complexity level. The GIM is included in the CD attached to the thesis report.

3.7.1 GUI-presentation

To initiate the GUI, the Matlab-code showed in algorithm 3.1 is compiled.

Algorithm 3.1 Initiating the graphical user interface of the GIM-model.

```
% Glucose-Insulin Simulator
global numprova numprova_n numprova_d numprova_d
warning off
clear all
numprova=1;
numprova_n=1;
numprova_d=1;
choose_status
```

The GUI is initiated and the following window is displayed:

[1] Graphical User Interface

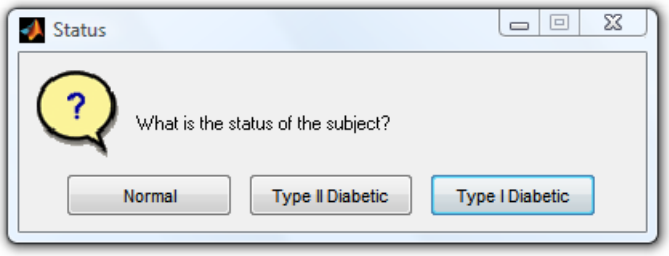

Figure 3.6: Simulating the GIM-model, step one.

The first window allows the user to choose the status of the subject. This way, the user is able to study the glucose-insulin dynamics in both normal and diabetic subject with the push of a button, rather than manually manipulating complex differential equations. Which demands a high level of understanding and competence related to mathematical modeling.

Since the focus in this thesis is to study the course of glucose and insulin in healthy subjects, the status "Normal" is chosen.

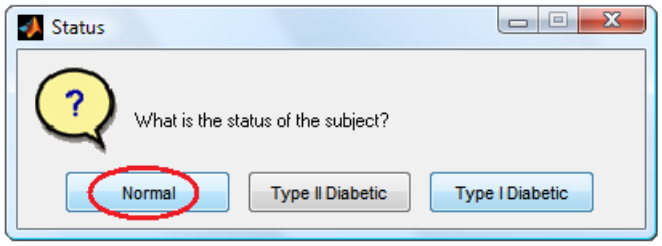

Figure 3.7: Simulating the GIM-model, step two.

After having chosen the status of the subject, the following window with default parameter values appear:

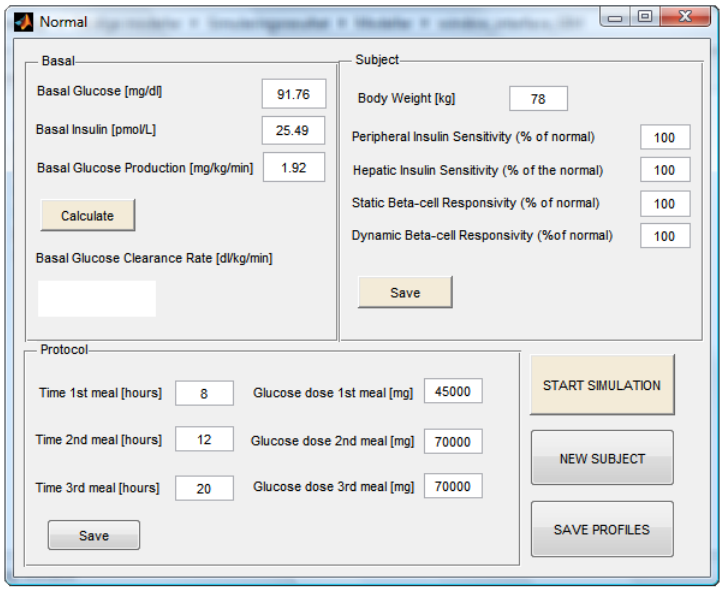

Figure 3.8: Simulating the GIM-model, step two.

Figure 3.8 enables the user to specify the parameters for the glucose-insulin simulation. Again, the GIM-models user friendliness is demonstrated. The user is able to specify basal glucose and insulin concentration, as well as basal glucose production. Figure 3.8 indicates additional parameters that can be specified eg. body weight, peripheral insulin sensitivity and dynamic β-cell responsivity. The GIM user interface also allow the user to specify the quantity of the glucose intake and at what time. In our case, 45 g is infused at time $t = 4$ hr, and 75 g at time $t = 10$ hr and $t = 17$, see figure 3.9.

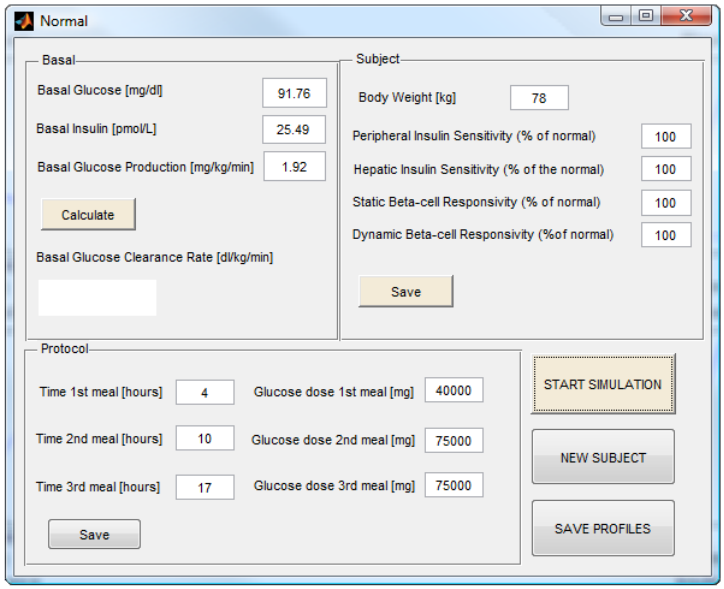

Figure 3.9: Specifying simulation parameter in the GIM GUI.

The simulation result is displayed when pushing the "START SIMULATION" button in figure 3.8.

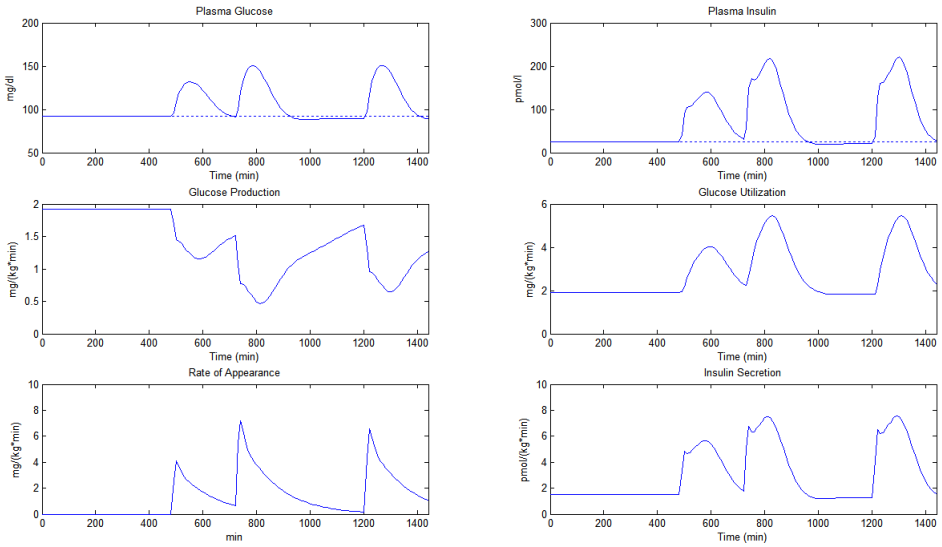

Figure 3.10: Simulation result of the GIM-model.

Figure 3.8 illustrate the output signals when the GIM-model is simulated. Plasma glucose and plasma insulin, the two top panels, are the two signal

used as reference in chapter 4. The output signal "Rate of Appearance" in the lower left hand corner represents the glucose input signal. Its form is somewhat deviating for the glucose input signal G_{inn} applied when simulation the other models. It is not possible to manually define the shape of this signal, just the infused glucose quantity and time of infusion.

All models have now been presented with their associated structural characteristics, differential equations and model parameters. They vary widely in in terms of complexity, assumptions and approach to model the glucoregulatory process. In the following, their ability to accurately simulate blood sugar control will be evaluated as they are implemented and simulated in Matlab and Simulink.

Chapter 4

Implementation and results

This chapter will present how the models are implemented in Matlab and Simulink. The simulation result of the models will be presented and compared, highlighting distinctive simulation characteristics in each of the models. Based on this, a modified model will be developed and presented.

4.1 Implementation

All models are implemented and simulated in Matlab[1] and Simulink[2]. In Simulink, function block are used to implement the differential equations. Each of the differential equation are implemented in separate function block to get a clear overview of input and output signals. The implementation of the S&H-model is presented as an example in figure 4.1:

[1] www.mathworks.se

[2] www.mathworks.se/products/simulink

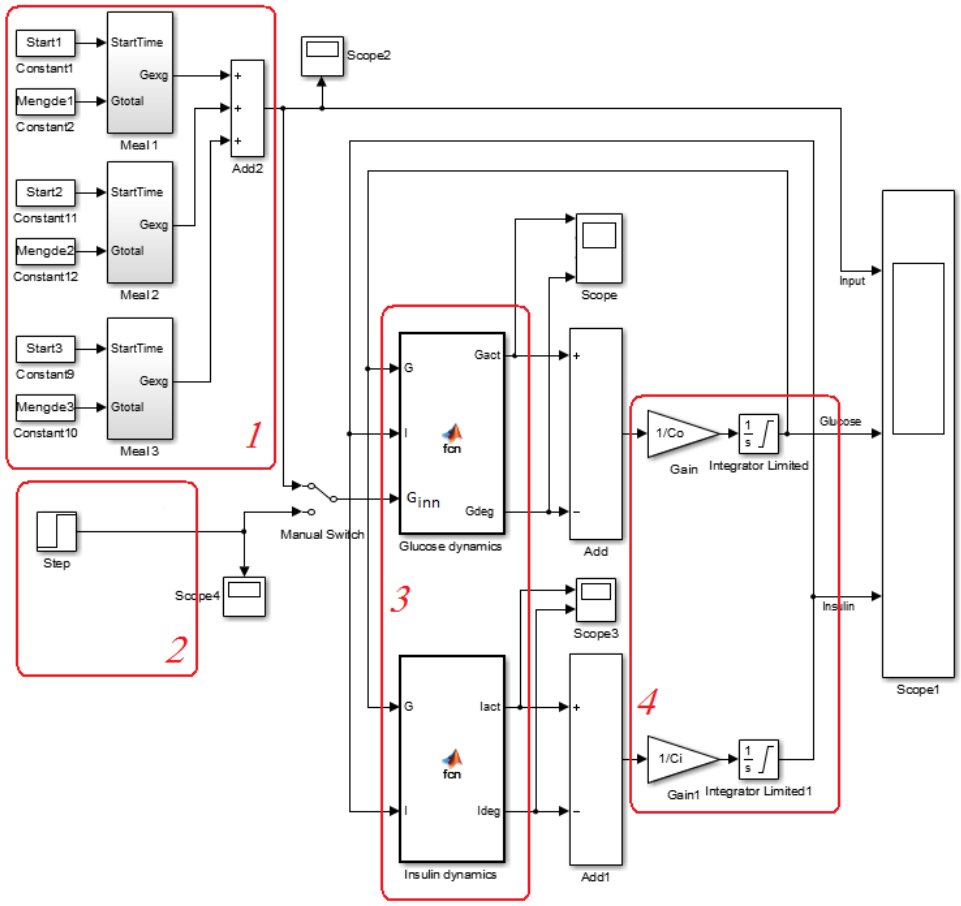

Figur 4.1: Simulink implementation of the S&H-model.

The model implementation presented in figure 4.1 contains the following four main segments marked in red:

1. Input signal applied to examine the glucose-insulin response to three meals over a time period of 24 hrs. The signal is based on the model of Fletcher and Yates [48], and infuses 40 g glucose at time $t = 4$, 75 g at $t = 10$ and 75 g at $t = 17$. The amount of glucose is based on the dosage given in oral glucose tolerance tests. The signal is displayed in figure 4.2.

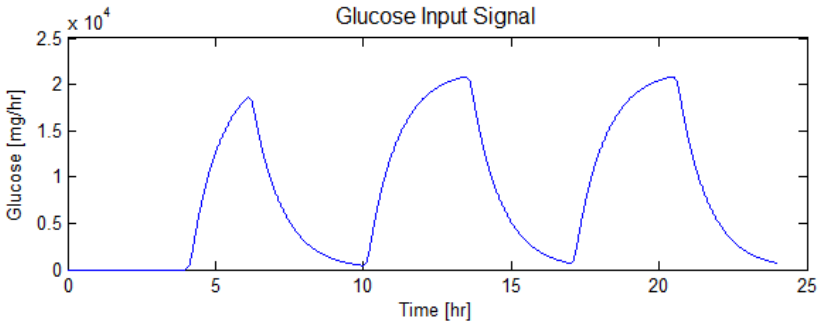

Figure 4.2: Input signal applied to examine glucose-insulin response to three meals.

The input signal in the GIM-model has a different shape, but the same glucose quantity is infused. This because the GUI inhibits the user in specifying the shape of the input signal. Only the glucose quantity and infusion time can be specified. The GIM-input signal is displayed in figure 4.3

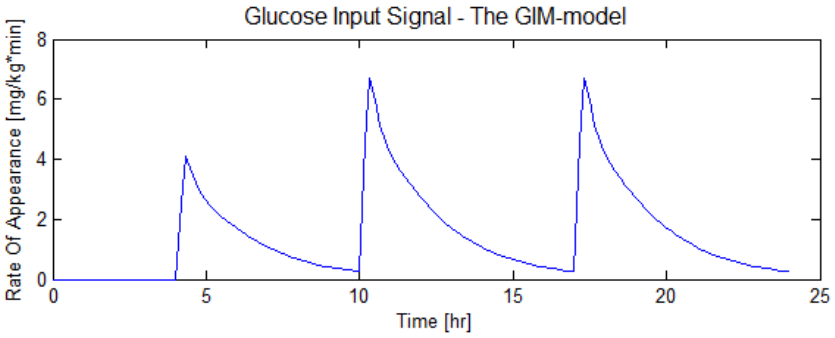

Figure 4.3: Glucose input signal of the GIM-model.

2. Input step-signal applied to examine homeostatic control properties in the models. The 10 g continuous glucose signal presented in figure 4.4.

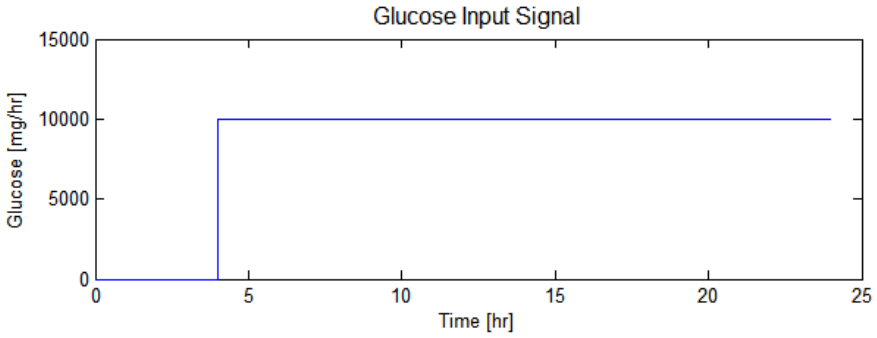

Figure 4.4: Common glucose input signals for each of the models to examine homeostatic control.

3. Simulink function-block implementation of the glucose- and insulin dynamics with their respective input/output signals.

4. The differential glucose- and insulin expressions are scaled and integrated resulting in the glucose and insulin output signal displayed in Scope 1. The simulation result is then imported in the Matlab workspace, and further scaled and plotted.

Simulink implementation for each of the models is presented in appendix C. In addition to the Simulink implementation, the simulation result was imported and processed in Matlab. This was needed as all the models were designed in different time scales and with different glucose- and insulin units as presented in table 4.1.

	Time	**Glucose**	**Insulin**
The GIM-model	[min]	[mg/dl]	[pmol/l]
The βIG-model	[day]	[mg/dl]	[μU/ml]
The βIGIR-model	[day]	[mg/dl]	[μU/ml]
The GIE-model	[min]	[mg/dl]	[ng/dl]
The S&H-model	[hr]	[mg/dl]	[μU/ml]
Chosen Simulation Units	**[hr]**	**[mg/dl]**	**[μU/ml]**

Table 4.1: Overview of model units.

The m-files initiating, scaling and plotting the simualtion for the two separate input signals is called “Response” and “Homeostasis” and is attached in appendix D. The simulation result is presented and discussed in section 4.2 and 4.3.

4.2 Glucose/Insulin response

To examine the physiological accuracy of the models, the glucose/insulin response to three meals is examined, applying signal 1. Their physiological accuracy will be discussed based on the GIM-reference simulation. The result is presented in a common plot for comparison, figure 4.5 and 4.6, followed by a more detailed presentation of the models individually.

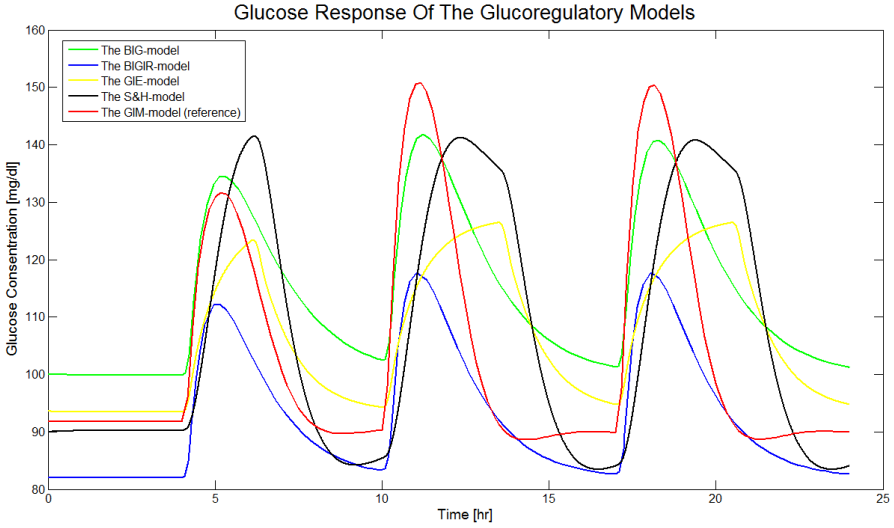

Figure 4.5: The glucose response for the separate models plotted together.

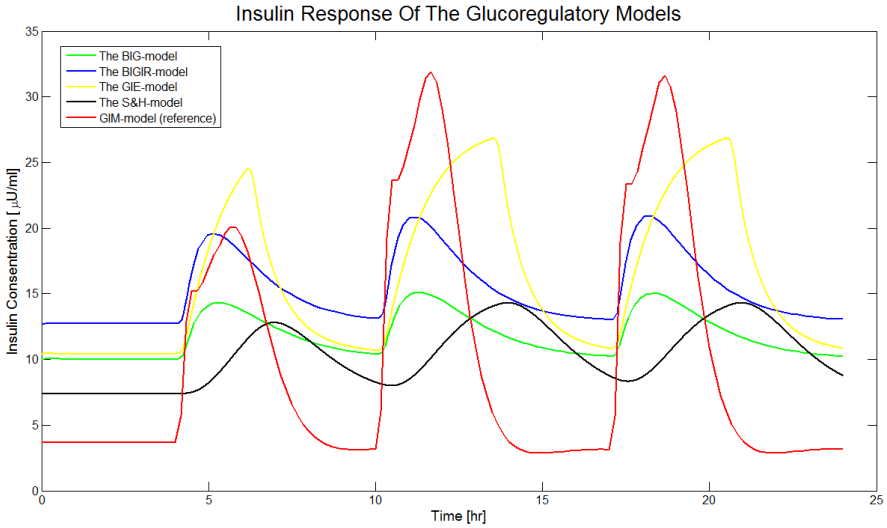

Figure 4.6: The insulin response for the separate models plotted together.

The simulation result of the BMM deviated strongly from the other models and is therefore plotted individually in figure 4.7.

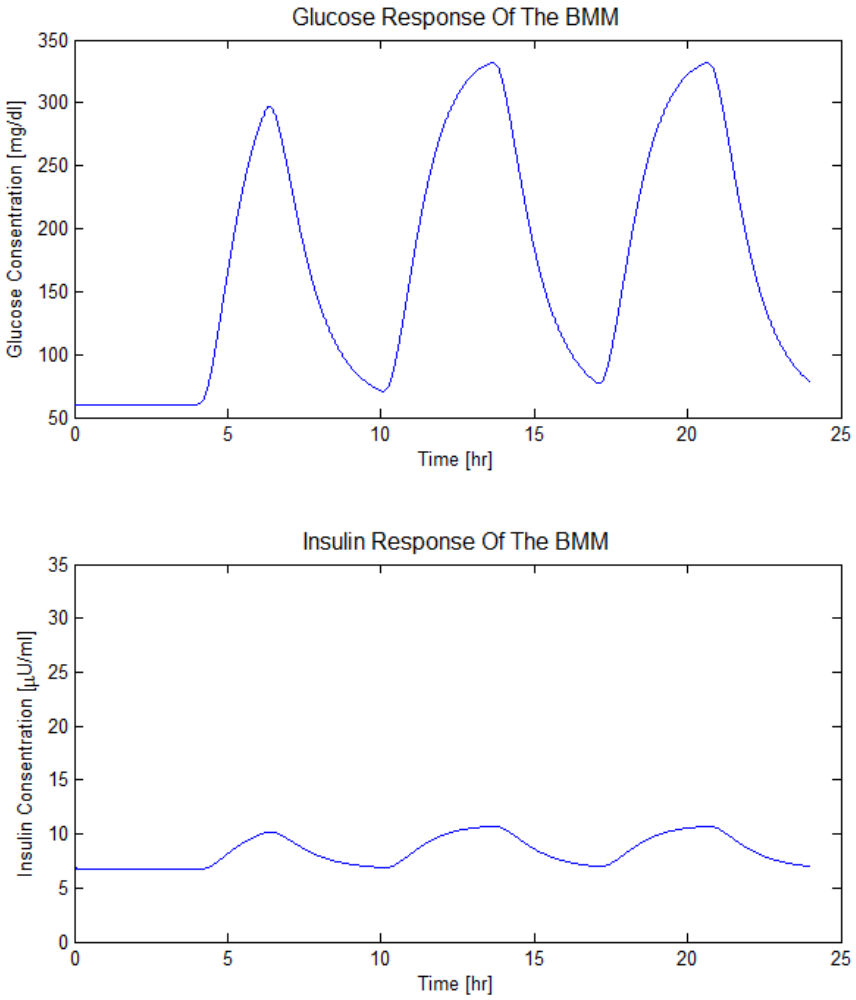

Figure 4.7: The BMM-simulation result plotted individually due to a markedly deviation form the other model simulation results.

Some key points for the simulation results are presented in table 4.2. For each of the response values, the best and weakest match, compared with the reference value, is indicated with green and red respectively. As the BMM-result deviated significantly form the others, it is examined on its own.

Response Value	OGTT (reference)	GIM (reference)	βIG	βIGIR	GIE	S&H	BMM
G_{basal} [mg/dl]		91.7	99.8	82.0	93.5	90.3	60.2
I_{basal} [μU/ml]		4.2	10.0	12.7	10.4	7.4	6.7
G_{40g} [mg/dl]		131.7	134.6	112.2	123.4	141.3	297.0
I_{40g} [μU/ml]		23.3	14.3	19.6	24.5	12.8	10.2
G_{40g}-I_{40g} ratio		108.4	120.3	92.6	98.9	128.5	286.8
$G_{75g,t=10}$ [mg/dl]		150.8	141.8	117.8	126.4	141.0	332.0
$I_{75g,t=10}$ [μU/ml]		36.9	15.1	20.9	26.8	14.3	10.7
G_{75g}-I_{75g} ratio		113.9	126.7	96.9	99.6	126.7	321.3
$G_{75g,t=17}$ [mg/dl]		150.4	140.8	117.8	126.4	141.0	332.0
$I_{75g,t=17}$ [μU/ml]		36.6	15.0	20.9	26.8	14.3	10.7
1 hr after 75 g oral glucose intake	$<$ 200 mg/dl	150.5	141.0	117.8	114.9	114.6	165.0
2 hrs after 75 g oral glucose intake	$<$ 140 mg/dl	130.1	135.0	108.6	123	139.9	278.5

Table 4.2: Key values in the glucose/insulin simulation results.

The over all aim of this simulation is to examine if the models simulate a healthy glucose-insulin response to the tree meals. This is verified or disproved by comparing the simulation result of each of the models to a reference response; the GIM-model. A quantitative reasonable response, in addition to homeostatic control examined in section 4.3, will be used as measure regarding the physiological validity of the models. In the following, the glucose/insulin response in each of the models will be evaluated, starting with the GIM-reference response.

.

4.2.1 The GIM-model

Figure 4.8 presents the GIM-simulation result to input signal displayed in figure 4.3, section 4.1.

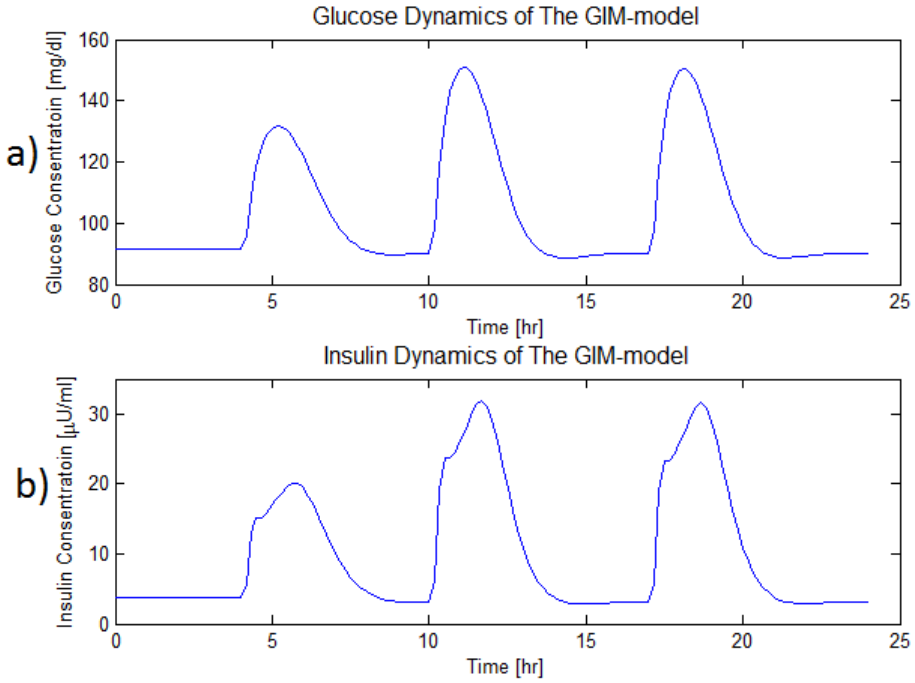

Figure 4.8: The glucose-insulin response of the GIM-model.

The GIM-model is a physiologically based model. It is developed considering the metabolic substrates at their intracellular organ/tissue level. Its complexity support its physiological plausibility and is therefor used as reference when considering the other, less complex models.

As mentioned in section 4.1, the input signal applied in the GIM-model has a different shape than the signal applied in the other model simulations. This because the user is unable to specify this input signal. The infused glucose quantity, and infusion time is however equal in both signals. The quantitative response is therefor comparable.

4.2.2 The Bergman Minimal Model

Figure 4.9 presents the simulation result of the BMM put in context with the GIM-reference. Numerical details of the simulation is presented in table 4.2.

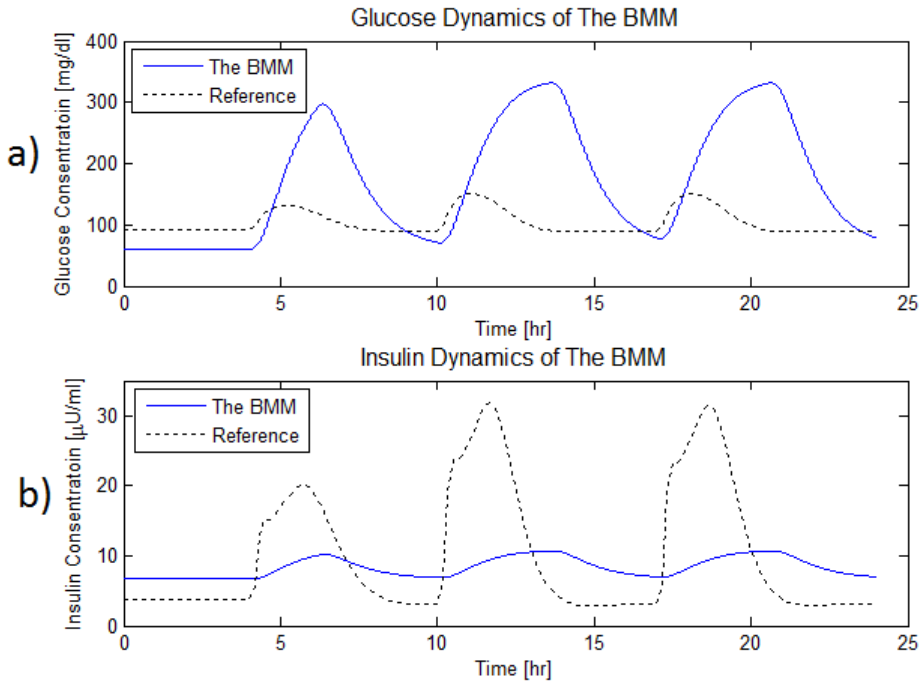

Figure 4.9: The glucose-insulin response of the BMM.

Comparing the two, the BMM show a overall higher glucose response, panel a), and a markedly lower insulin response, panel b). The simulation illustrates the short comings in the model due to its limited complexity and simplifying assumptions. However, the BMM is well established in the field of biochemical modeling, and is the most frequently cited of the ones examined. Its seemingly poor simulation result can therefor be linked to, and caused by errors in the simulation process, and not necessarily the model itself. Inconsistent use of input signal, scaling error and model adjustment are mention as possible sources of errors.

The empirical BMM is designed based on a systems input/output relationship, not focusing on details within the system itself. The drawbacks of this is that the simulation result show limited physiological validity, cf figure 4.9.

Minimal models are however valuable stating points regarding model modification and optimization. The βIG-model is designed based on the BMM and is presented in the following.

4.2.3 The βIG-model

The simulation result of the βIG-model plotted together with the GIM-reference simulation is presented in figure 4.10.

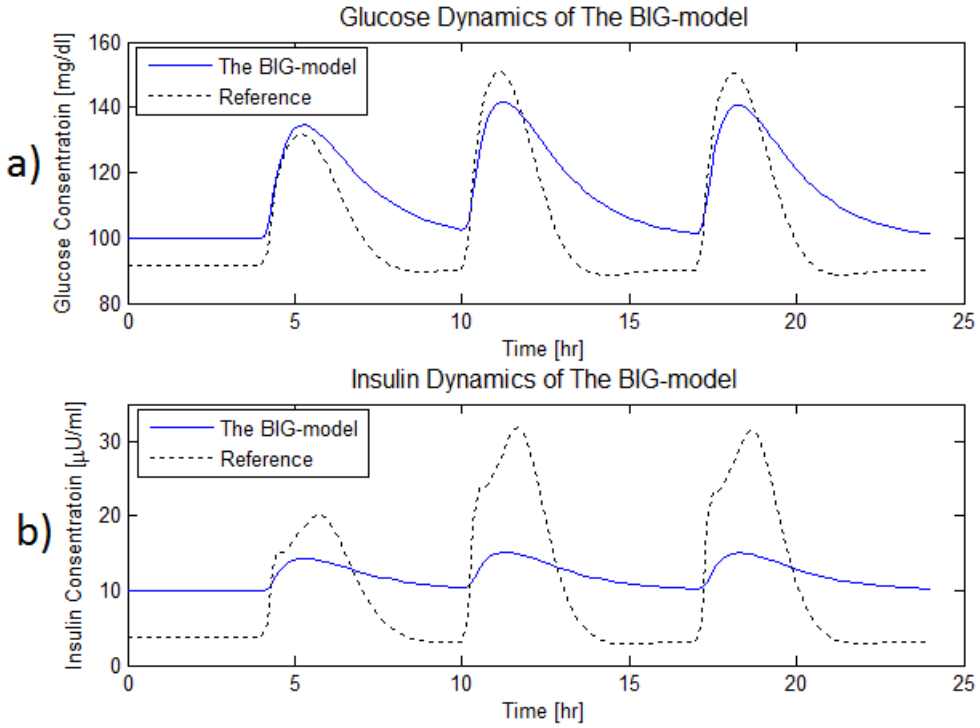

Figure 4.10: The glucose-insulin response of The βIG-model.

Figure 4.10, panel a) illustrates that the βIG-model simulates a adequate glucose response compared to the GIM-reference response. The βIG-model includes the dynamics of β-cell mass and has a more complex insulin secretion flux than the BMM. This seemingly improves the models ability to simulate healthy glucose response.

Even though figure 4.10 illustrates a more physiological reasonable quantitative glucose response than the BMM, the glucose/insulin *ratio* is more questionable. Panel b), figure 4.10 illustrate a markedly lower insulin response than the stippled reference value. It is therefor interesting how such a

low insulin level is able to correspond to such a reasonable glucose response. Thus the glucose response can be anatomically justified, but the glucose/insulin ration limits the physiological validity of the model. The parameter estimation and -fitting regarding the glucose dynamics is therefor seemingly more successful than for the insulin dynamics.

4.2.4 The βIGIR-model

Figure 4.11 presents the βIGIR-model simulation result.

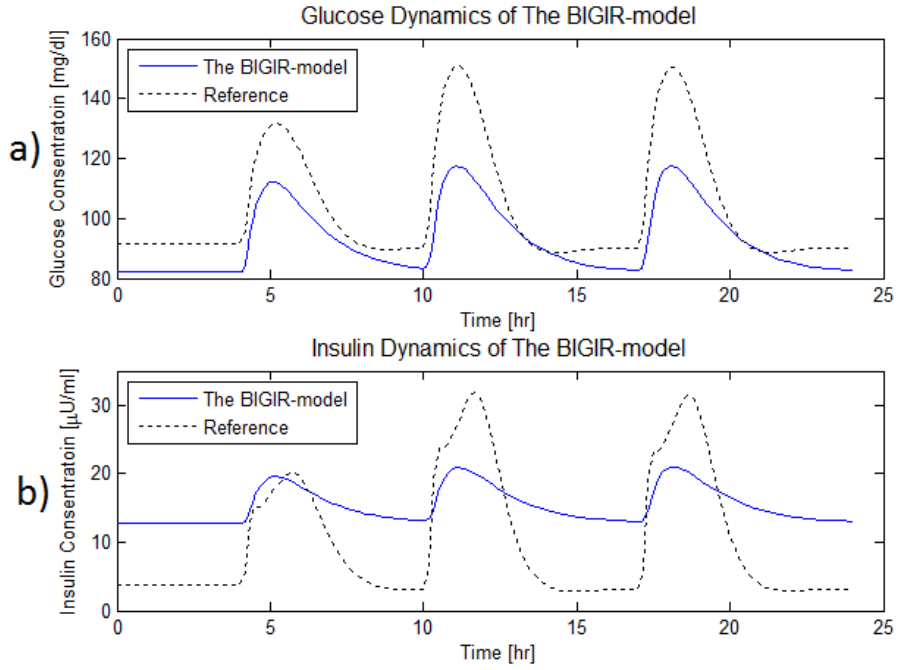

Figure 4.11: The glucose-insulin response of The βIGIR-model.

The βIGIR-model is a modification of the βIG-model including the dynamics of muscle insulin receptors. It aims to simulate how normal blood sugar levels can be maintained in spite of reduced insulin sensitivity. As a result of the reduced insulin sensitivity, the plasma insulin concentration must be higher to maintain normal glucose control, see figure 4.11, panel b). This high insulin concentration result in a lower glucose concentration than the one seen in the βIG-model. This signalize a reasonable connection between the glucose- and insulin response, but the numerical simulation result is over all significantly lower than the reference.

In line with the BMM and the βIG-model, the βIGIR-model is a empirical minimal model. The simulation performance is therefor strongly linked to parameter estimation and -assignment. The fact that the simulation result shows a overall low glucose- and insulin response is mainly linked to the insulin receptor dynamics. It addresses a special case within blood sugar regulation, which limits its general anatomical validity and applicability. The impression of the model quality is also affected negatively by the glucose response. This should be closer linked to the GIM-reference response as it aims to simulate healthy glucose control. Figure 4.11, panel a) illustrate a significant deviation between the two.

4.2.5 The GIE-model

The GIE-simulation result is presented in figure 4.12.

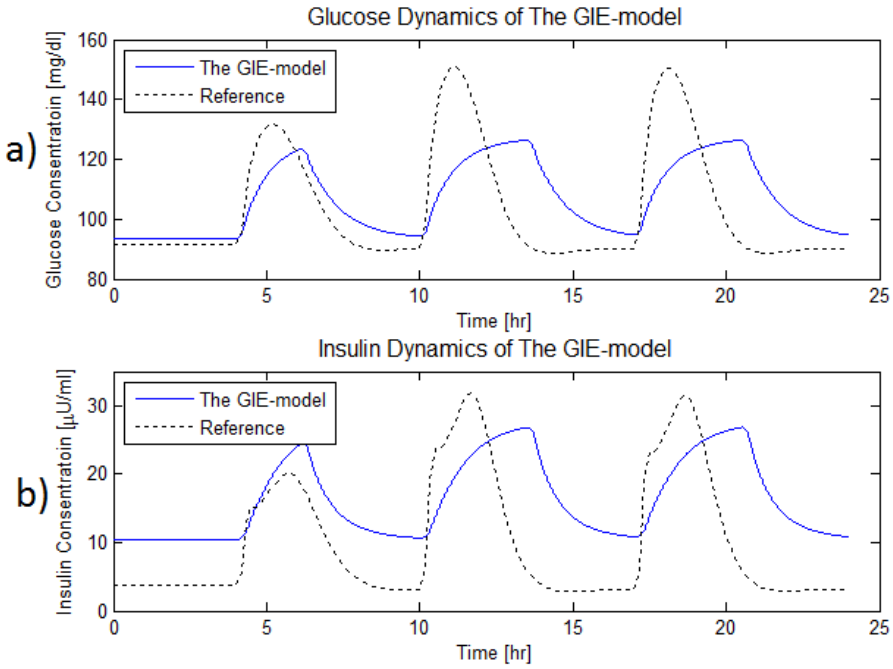

Figure 4.12: The glucose-insulin response of the GIE-model.

Apart from the GIM-model, the GIE-model is the most complex of the ones examined. Despite its mathematical complexity, the simulation result displayed in figure 4.12 show both a glucose- and insulin response quite deviating form the reference. The shape of the GIM-response curves is strongly resembling the glucose input signal, see figure 4.2 section 4.1. This is seemingly

linked to the mathematical complexity of the model. As the shape of the GIM-input signal is different from the GIE-input signal, the shape of the response is logically different. Their numerical response values however. should be more alike as the glucose quantity in both the signals is the same.

The GIE-model is a semi-empirical model. Compared with the strictly empirical models, it is designed with a stronger focus on the anatomical system as such, rather than simply describing a input/output relationship. It should therefor be able to simulate a glucose and insulin response closer related to the stippled reference curves. The threshold functions, and weakly estimated threshold values can be part of the limitation in the simulation result. Poor parameter estimation and parameter fitting can also affect the model performance negatively.

4.2.6 The S&H-model

Figure 4.13 illustrates the S&H-simulation result.

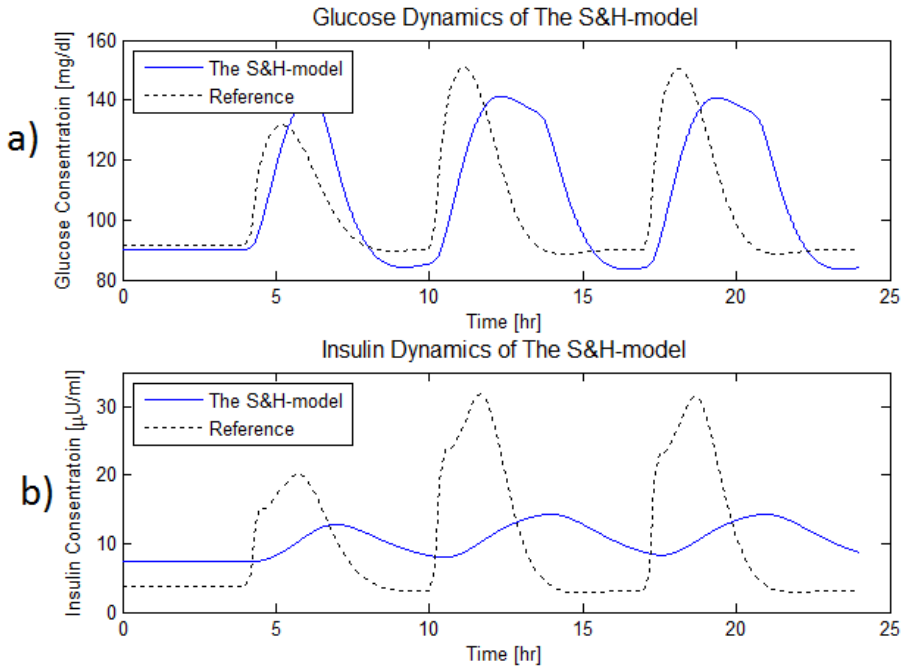

Figure 4.13: The glucose-insulin response of the S&H-model.

The glucose response displayed in panel a) is closely resembling the stippled reference curve. The insulin response, panel b), is however significantly lower.

It is reasonable to think that such a low insulin level would cause a higher glucose concentration curve, as seen in the BMM-simulation. The glucose level is within an anatomically reasonable range in spite of a low insulin concentration. Thus the S&H-model simulates a physiological reasonable glucose response, but a less reasonable glucose/insulin ratio.

The insulin response is time shifted relative the glucose dynamics curve. This is also seen in the GIM-reference simulation. It is reasonable to think that the insulin secretion is delayed relative the blood sugar elevation. The model captures a physiological justifiable phenomenon. Being a strictly empirical model, the accurate glucose response and time shifted insulin response is presumably the result of fortunate parameter estimation and threshold value assignment.

4.3 Homeostasis

Homeostatic control is achieved if the steady state glucose concentration approaches its initial fasting level, even at a continuous glucose intake. To examine the homeostatic property of the models, a low continuous input signal of 10 g glucose is applied, displayed in figure 4.4 section 4.1. The simulation result is displayed in figure 4.14. All model simulations are plotted together for comparison, and with the GIM-model as reference.

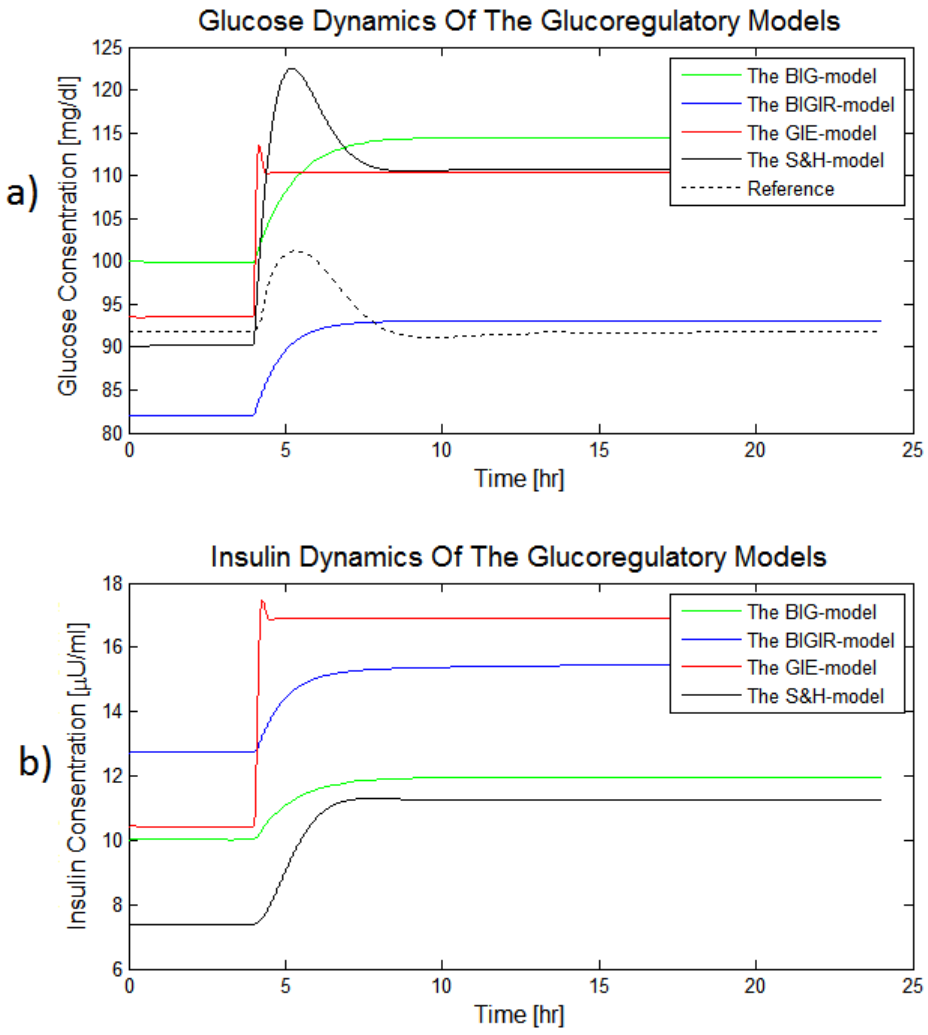

Figure 4.14: Simulation result when a continuous low glucose input signal is applied.

Again, the BMM simulation is quite deviating from the rest. It is therefore

plotted separately from the other models in figure 4.15.

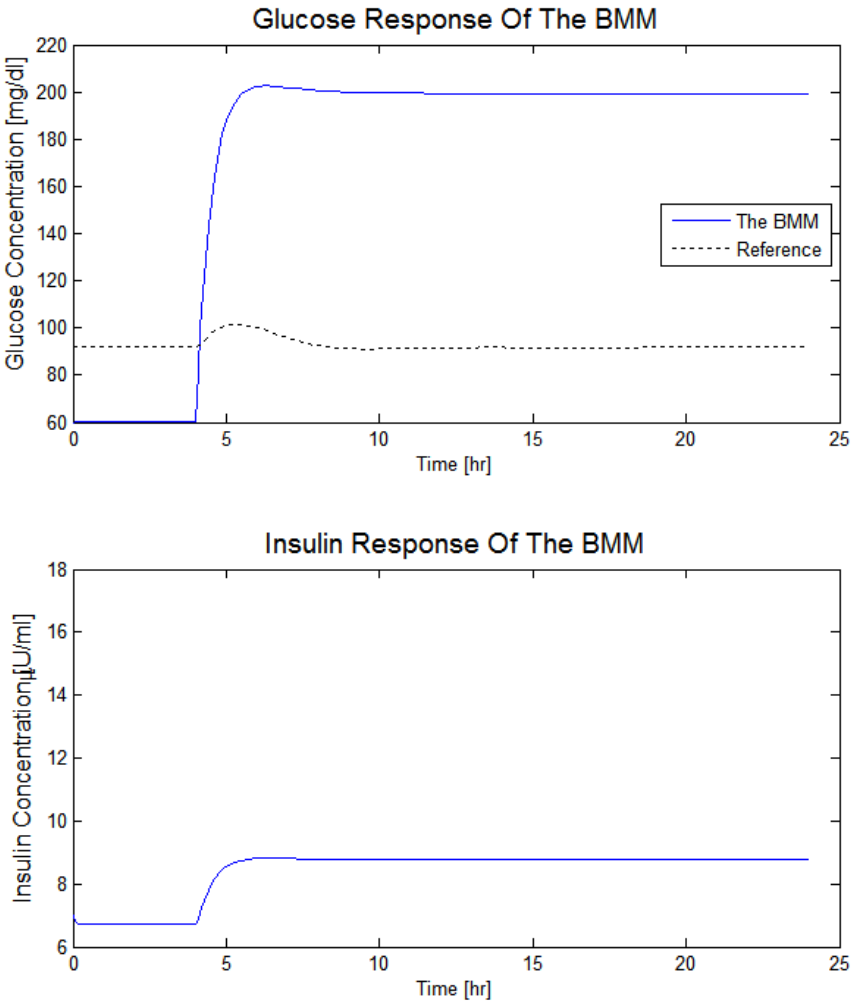

Figure 4.15: Simulation result of the BMM when a continuous low glucose input signal is applied.

The GUI of the GIM-model does not allow the user to specify the shape of the input signal. It is therefore not possible to define a continuous low glucose input signal to examine the homeostatic property of the model. The GIM-model is used as a illustration of how a homeostatic glucose response would look like. Figure 4.14 and 4.15 implies that none of the models are able to simulate homeostatic control. To examine this more in detail, the models are reviewed individually starting with the BMM.

4.3.1 The BMM

The simulation result of the BMM, figure 4.15, show no homeostatic glucose control. In addition, the glucose response to the 10 g infused glucose is semmingly unrealistically high. This combined with a very low insulin response limits the over all anatomical plausibility of the BMM.

Models with auto catalysis, zero-order degradation terms or Michaelis-Menten enzyme kinetics is assumed to simulate physiologic integral control. The BMM has zero order degradation of both insulin $I(t)$, and remote insulin in action $X(t)$, cf. eq. 4.1 and 4.2 respectively.

$$\frac{dI(t)}{dt} = nI_b - nI(t) + \gamma G(t) - \gamma \mathbf{h} \tag{4.1}$$

$$\frac{dX(t)}{dt} = p_3 I(t) - p_2 X(t) - \mathbf{p_3 I_b} \tag{4.2}$$

Based on equation 4.1 and 4.2 the following steady state expressions are derived:

$$\frac{dI(t)}{dt} = nI_b - nI(t) + \gamma G(t) - \gamma h = 0$$

$$G(t)_{SS} = \frac{\gamma h + nI(t) - nI_b}{\gamma}$$

$$\mathbf{G(t)_{SS}} == \mathbf{h} + \frac{\mathbf{n}}{\gamma}\left(\mathbf{I(t)} - \mathbf{I_b}\right) \tag{4.3}$$

$$\frac{dX(t)}{dt} = p_3 I(t) - p_2 X(t) - p_3 I_b = 0$$

$$I(t)_{SS} = \frac{p_2 X(t) + p_3 I_b}{p_3}$$

$$\mathbf{I(t)_{SS}} = \frac{\mathbf{p_2}}{\mathbf{p_3}}\mathbf{X(t)} + \mathbf{I_b} \tag{4.4}$$

Expression 4.3 and 4.4 presents the glucose- and insulin steady state expressions as functions of variables. To achieve homeostatic control, the steady state glucose concentration must approach a numerical value. This is seemingly prevented when the steady state expression is a function of a time varying variable. The BMM illustrate how zero-order degradation in *combination* with degradation of first order prevent homeostatic control.

4.3.2 The βIG- and βIGIR- model

Considering figure 4.16, neither the βIG- nor the βIGIR-model simulates homeostatic glucose control when simulated for 24 hrs. The glucose level is merely stabilized at a higher.

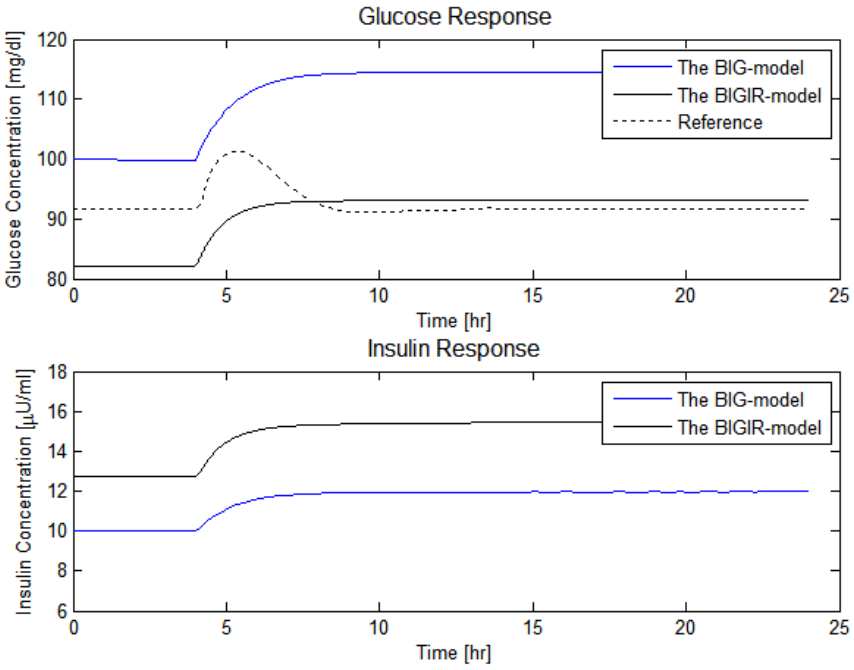

Figure 4.16: The glucose/insulin response of the βIG- and βIGIR-model to a continuous low glucose input.

This seemingly contradicts the hypothesis of auto catalysis causing integral control, as both models have auto catalyzed β-cell mass dynamics:

$$\frac{d\beta(t)}{dt} = \left(-g + hG(t) - iG(t)^2\right)\beta(\mathbf{t}) \tag{4.5}$$

Based on equation 4.5, the steady state glucose expression is derived:

$$\frac{d\beta(t)}{dt} = \left(-g + hG(t) - iG(t)^2\right)\beta(t) = 0$$

$$iG(t)^2 - hG(t) + g = 0 \tag{4.6}$$

Solving equation 4.6 result in the following steady state glucose concentration G_{SS}:

$$G_{SS} = \frac{h \pm \sqrt{(-h)^2 - 4ig}}{2i} \tag{4.7}$$

Where $(-h)^2 - 4ig > 0$ result in two equilibrium points for the steady state glucose concentration $G(t)$. Expression 4.7 implies integral control of the steady state glucose concentration $G(t)$. As the time scale of the models is days, slow process dynamics is assumed. Thus the models must be simulated over a longer time period than 24 hrs to illustrate the homeostatic control property. Figure 4.17 illustrates the simulation result of the two models when simulated for 500 days.

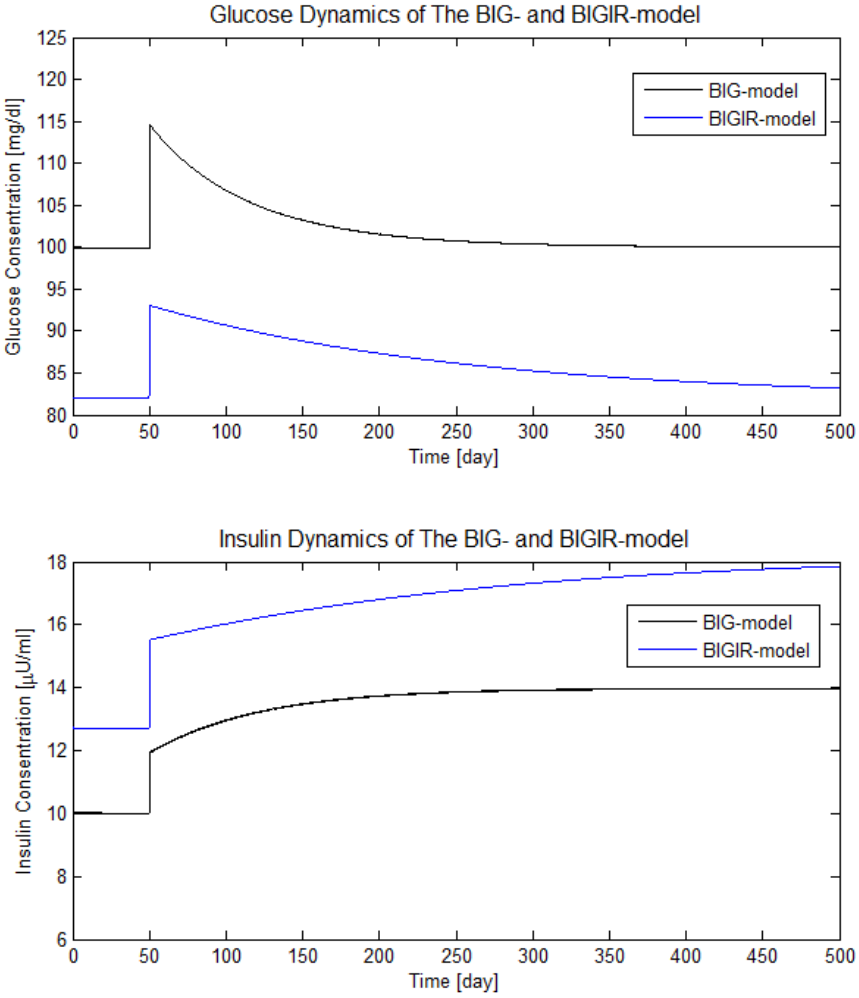

Figure 4.17: Simulation result of the βIG- and βIGIR-model showing homeostatic control.

Figure 4.17 illustrates that auto catalysis can improve the models ability to capture homeostatic control. The fact that is takes 500 day has however no correlation with reality.

4.3.3 The GIE- and S&H-model

Figure 4.18 illustrate how neither the GIE-model nor the S&H-model is able to simulate physiologic glucose control. The stippled line illustrate how the glucose concentration qualitatively should look like.

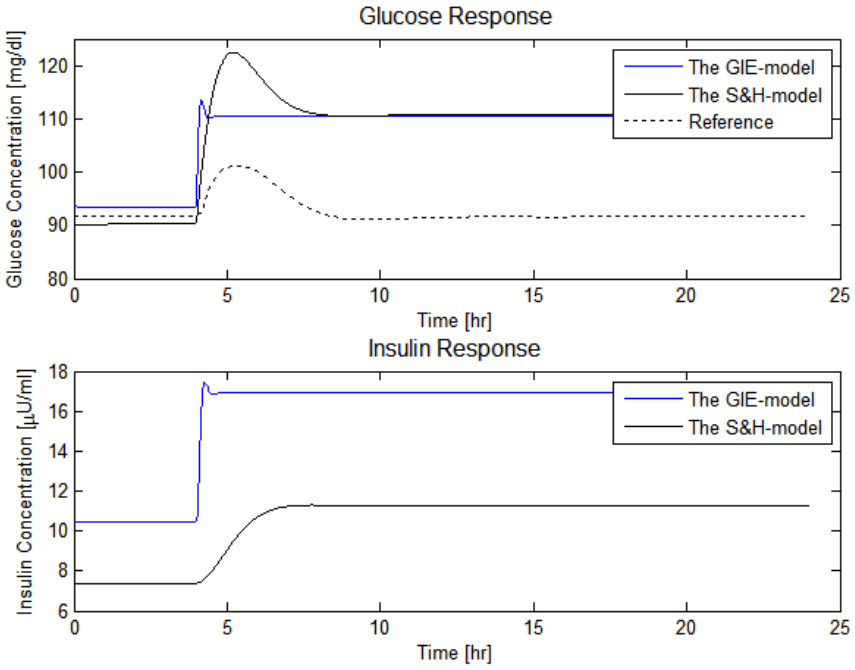

Figure 4.18: The glucose/insulin response of the GIE- and S&H-model to a continuous low glucose input.

The two models are markedly different regarding mathematical complexity. The GIE-model comprises three higher order, nonlinear differential equations. Its description of the glucose dynamics is made up of seven terms including threshold functions and complex enzyme kinetics. Whereas the S&H-model describes blood sugar regulation using only two differential equations with simple enzyme kinetics. It is therefor more reasonable that the S&H-model is unable to simulate glucose homeostasis than the GIE-model.

As earlier stated, zero-order degradation or auto catalysis can ensure physiologic integral control. All terms in the GIE-model is of first order or higher. In line with the BMM, the S&H-model has a zero-order insulin degradation term, in combination with a degradation term of first order. This is presumably the reason why homeostatic control is prevented in both models.

4.4 Model optimization

Minimal models with their limited complexity are well suited for further development and optimization. This will be demonstrated in the following as the empirical S&H-minimal model is modified. The aim of this modification is to improve the S&H-simulation performance regarding homeostatic glucose control. This modification will *principally* illustrate how homeostatic control can be achieved. Numerical details is less of a focus point. The original S&H-model is presented in eq. 4.8 and 4.9.

$$C_G \frac{dG(t)}{dt} = Q - \gamma I(t)G(t) - \delta G(t) - \mu \left(G(t) - G_K\right) \tag{4.8}$$

$$C_i \frac{dI(t)}{dt} = -\alpha I(t) + \beta \left(G(t) - G_0\right) \tag{4.9}$$

The approach is to introduce zero order insulin degradation. The degradation rate α in equation 4.9 is no longer dependent of the insulin concentration $I(t)$. The modified model, referred to as the S&H*-models, then becomes.

$$C_G \frac{dG(t)}{dt} = \left(Q - \gamma I(t)G(t) - \delta G(t)\right) \tag{4.10}$$

$$C_i \frac{dI(t)}{dt} = \left(\beta \left(G(t) - G_0\right) - \alpha\right) \tag{4.11}$$

Based on eq. 4.11, the glucose steady expression is derived:

$$\left(\beta \left(G(t) - G_0\right) - \alpha\right) = 0$$

$$G(t) = \frac{\alpha}{\beta} + G_0$$

The parameter G_0 is a threshold value presumably defined by Stolwijk and Hardy to optimize the simulation result. The G_0 threshold can therefore be adjusted to optimize the simulation result in the modified model. It is desired

that the glucose concentration $G(t)$, at steady state, equals the initial glucose level of 90.28 mg/dl. The threshold parameter is assigned the following value:

$$\frac{\alpha}{\beta} + G_0 = 90.28$$

$$G_0 = 90.28 - \frac{76.0}{14.3} = 84.69 \approx 85$$

The modified model with zero-order degradation and adjusted threshold value is implemented and simulated. The same continuous 10 g glucose input signal is applied. The result is displayed in figure 4.19.

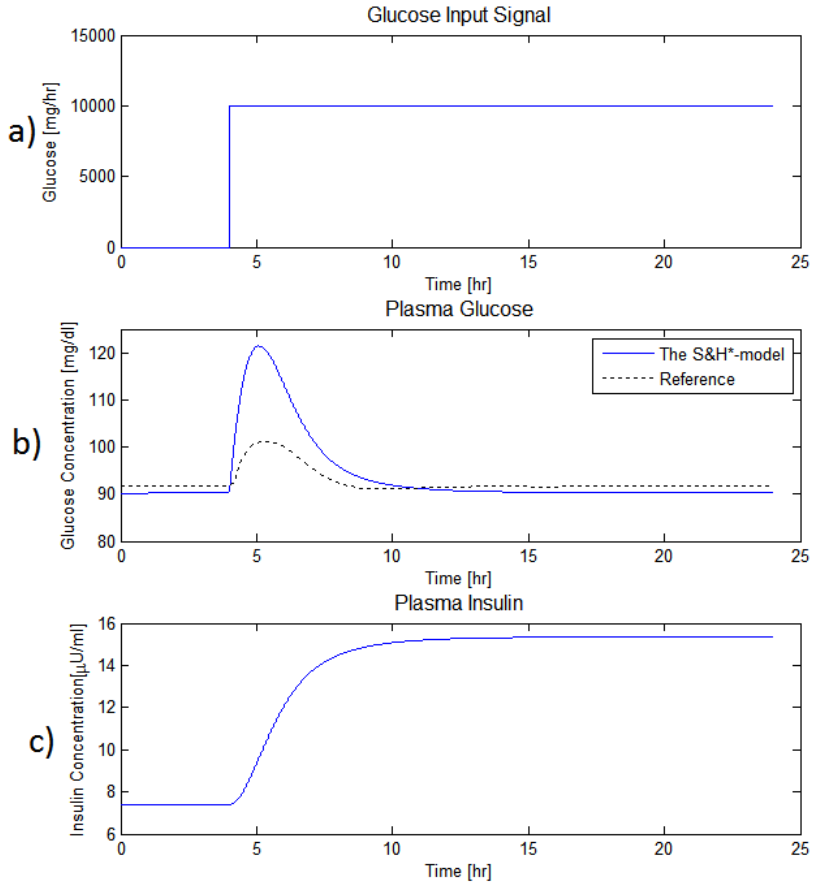

Figure 4.19: Simulation result of the optimized model.

Figure 4.19, panel b) illustrate how the modified model is able to simulate a controlled steady state glucose concentration. This in spite of a continuous glucose infusion illustrated in panel a). The numerical simulation result

was however quite divergent from the GIM-reference. The main aim of the model modification was to illustrate how a zero-order insulin degradation would improve the homeostatic control property in the S&H-model, which was done satisfactorily.

Chapter 5

Discussion and conclusion

5.1 Conclution

In this thesis, six of the most cited mathematical models of the glucoregulatory system have been examined. The examination has focused on studying the models' glucose-insulin oscillation related to fool intake, and their ability to simulate homeostatic glucose control.

The simulation result showed that only two out of the six models, the βIG- and βIGIR-model, were able to indicate physiological integral control of the steady state glucose concentration. This was presumably linked to the auto catalyzed β-cell mass in the two models. To maintain glucose homeostasis is supposedly the most important task of glucose control. The fact that the BMM, GIE- and S&H-model were unable to simulate this property limits their physiological plausibility and -validity. This can possibly be explained by their lack of zero-order degradation terms, Michaleis-Menten approximation, auto-catalysis, simplifying assumptions, parameter fitting/-estimation or limited model complexity.

The BMM and S&H-model are however well established and often cited minimal models. They are used as foundation in design, modification and optimization of glucoregulatory models. The fact that they are seemingly unable to simulate glucose homeostasis can be linked to the input signal applied in the simulation. This signal is defined by yours truly, deviation from the glucose input signal defined in the model description and design process. This to apply a signal common for all models so they are studied on common grounds. The weak simulation result of the BMM and S&H-model regarding homeostatic control can therefore be the cause of a modeling error.

The simulation result of the six models, excluding the GIM- and the BMM, illustrated the strengths of the minimal models. With limited complexity they were still able to model glucose-insulin oscillation within an anatomically reasonable range. The least complex S&H-minimal model had simulation result of the glucose dynamics well corresponding to the result of the markedly more complex GIE-model. This implies that minimal models can be valuable in describing glucose-insulin regulation as they are compact, comprehensible and easier to apply and modify than more complex models.

The close correspondence in the simulation result of the two models can however be related to fortunate chosen input signal. This can be verified or disproved repeating the simulation with different glucose input signals.

The modification of the S&H-model, resulting in the S&H*-model, illustrated the principle of how zero-order insulin degradation may contribute to improver homeostatic model property.

It was also shown, in the BMM simulation, how zero-order insulin degradation *in combination* with an insulin degradation term of first order seemingly prevent homeostatic glucose control.

5.2 Further work

In this thesis, the glucose-insulin control of healthy subjects has been the focus point. Further work could therefore involve a similar model study of diabetic glucose-insulin control. To introduce PID-controllers when considering glucose-insulin regulation is also an interesting scenario. An interesting task would also be to develop a graphical user interface, as seen in the GIM-model, to make the complex models more comprehensible and unfriendly to those with limited modeling competence.

Maybe the most valuable suggestion to further work is however to improve the models' ability to simulate glucose homeostasis. Several suggestions to how this can be done have been presented. With improved model performance, in terms of homeostatic simulation, glucoreguatory models can be applied on a higher level of research which in turn may contribute to medical progression and innovation.

Bibliography

[1]

[1] The Norwegian diabetes association: http://www.diabetes.no/no/Om_diabetes/

[2] The American Diabetes Association, Diabetes Statistics: http://www.diabetes.org/diabetes-basics/diabetes-statistics/

[3] The American Diabetes Association, The Cost of Diabetes: http://www.diabetes.org/advocate/resources/cost-of-diabetes.html

[4] Fabhi Mohammed Ahmed Al-Akwaa, "The dynamic of glucose-insulin endocrine metabolig regulatory system: A system dynamics approach", Master thesis, Egypt March 2006.

[5] Homeostasis: http://www.biologyreference.com/Ho-La/Homeostasis.html

[6] Blood sugar regulation: http://www.biologyreference.com/Bl-Ce/Blood-Sugar-Regulation.html

[8] T.drengstig, I. W. Jolma, K. Thorsen og P. Ruoff, "Fysiologiske Reguleringsmekanismer".

[9] Diabetes mellitus: http://sml.snl.no/diabetes_mellitus

[11] Cecilia Brännmark, "Insulin Signaling in Human Adipocytes, A System Biology Approach", Sweden 2012.

[12] Diabetes mellitus type 1: http://sml.snl.no/diabetes_mellitus

[13] Diabetes mellitus type 2: http://sml.snl.no/diabetes_mellitus

[14] Hypoglycemia: http://en.wikipedia.org/wiki/Hypoglycemia

[15] Hyperglycemia: http://en.wikipedia.org/wiki/Hyperglycemia

[16] Islet of Lagerhans: http://en.wikipedia.org/wiki/Islets_of_Langerhans

[18] Arne Gunnar G. Jørgensen, "Modeling of Biochemical Reaction Networks", Stavanger 2009.

[19] Horton, Moran, Scrimgeour, Perry, Raw, "Principles of Biochemistry" 4th. edition, 2006.

[20] Enzymes: http://www.biologyreference.com/Dn-Ep/Enzymes.html

[21] Elimination of alcohol: http://www.forcon.ca/learning/alcohol.html

[22] Reaction boundaries figure: http://en.wikipedia.org/wiki/Michaelis%E2%80%93Menten_ki

[23] Tormod Drengstig, "Enzyme kinetics", Stavanger 2013.

[24] T. Drengstig, I. W. Jolma, X. Y. Ni, K. Thorsen, X. M. Xu, and P. Ruoff, "A Basic Set of Homeostatic Controller Motifs", Stavanger 2012.

[24] Insulin and Glucagon: http://sml.snl.no/insulin, http://sml.snl.no/glukagon

[25] Image of an insulin molecule: Insulin: http://en.wikipedia.org/wiki/Insulin

[26] Image of a glucagon molecule: Glucagon: http://en.wikipedia.org/wiki/Glucagon

[27] Pancrease: http://sml.snl.no/bukspyttkjertelen (http://en.wikipedia.org/wiki/Pancreas)

[28] Image of the pancreas: http://www.webmd.com/digestive-disorders/picture-of-the-pancreas

[29] Computional Biology group (CoBi), "Mathematical Modeling in Systems Biology", Zyrich.

[30] Dalla Man, Raimondo, Rizza, Cobelli, "GIM, Simulation Software of Meal Glucose-Insulin Model", Journal of Diabetes Science and Technology Vol. 1, May 2007.

[31] Kristian Thorsen, "Simulation Model of the Glucose-Insulin System, a University of Stavanger presentation", Stavanger 2012.

[32] Meier, Veldhuis, Butler, "Pulsatile Insulin Secretion Dictates Systemic Insulin Delivery by Regulating Hepatic Insulin Extraction In Humas", Diabetes Vol 54, June 2005.

[33] Dalla Man, Camilleri, Cobell, "A Sysem Model of Oral Glucose Absorbtion: Validation on Gold Standard Data", IEEE Transactions on Biochemical Engineering Vol 53 No 12, December 2006.

[34] Secretion of glucose through urine - Glucosuria. http://en.wikipedia.org/wiki/Glycosuria

[36] Sulston, Ireland, Praught, "Hormonal Effect on Glucose Regulation", Jurnal of Mathematics, Vol.1 No.1, 2006.

[37] The Bolier model: http://jap.physiology.org/content/16/5/783.short

[38] Roy Anirban, "Dynamic modeling Of Free Fatty Acid, Glucose and Insulin During Rest and Exercise in Insulin Dependent Diabetes Mellitus Patients", University of Pittsburg, 2008.

[39] Quote, Roy Anirban, "Dynamic modeling Of Free Fatty Acid, Glucose and Insulin During Rest and Exercise in Insulin Dependent Diabetes Mellitus Patients", University of Pittsburg, 2008, page 9, line 11.

[40] Friis-Jensen Espen, "Modeling and Simulation of Glucose-Insulin metabolism", Technical University of Denmark, 2007.

[41] Andersen, Højbjerre, "A Bayesian Approach to Bergman's Minimal Model", Alborg University, Denmark.

[42] Topp, Promislow, deVries, Miura, Finegood, "A Model of β-cell Mass, Insulin and Glucose Kinetics: Pathways to Diabetes", J. theor. Biol., 2000

[43] Quote, Topp, Promislow, deVries, Miura, Finegood, "A Model of β-cell Mass, Insulin and Glucose Kinetics: Pathways to Diabetes", J. theor. Biol., 2000, page 608, line 19

[43] Hernandez, Lyles, Rubin, Voden, Wirkus,"A Model of β-cell Mass, Insulin, Glucose And Receptor Dynamics With Applications To Diabetes", Cornell University, 2001

[44] Stolwijk and Hardy, "Regulation and Control in Physiology", Medical Physiology 13'th edition, 1974

[45] Quote, Stolwijk and Hardy, "Regulation and Control in Physiology", Medical Physiology 13'th edition, page 1354, collum 2, line 36

[46] SI unit conversion: http://www.soc-bdr.org/rds/authors/unit_tables_conversions_and_genetic_dictionaries/e5196/index_en.

[47] Kerry Walk, "How to Write a Comparative Analysis", Harvard University, 1998

[48] Yates, Fletcher, "Prediction of a glucose apperance function from food using deconvolution", J. Appl. Math. Med. Biol. 17, 2000

[49] Bergman, Ider, Bowden, Cobelli, "Quantitative estimation of insulin sensitivity", American Journal of Physiology, 1979

[50] Celeste, Ackerman, Gatewood, Reynolds, Molnar, "The role of glucagon in the regulation of blood glucose model studies", Math. Biol. 40, 1978

[51] Summers, Montani, "Mathematical model of glucose homeostasis for the study of metabolic states", J. Mississippi Acad. Sci. 34, 1989

[52] Summer, Montani, Woodward, Coleman, Hall, "Theoretical analysis of the mechanisms of chronic hyperinsulinemia", Comput. Biol. Med. 27, 1997

[53] Sturis, Polonsky, Mosekilde, Cauter, "Computer model for mechanisms underlying ultradian oscillations of insulin and glucose", Am. J. Physiol. 260, 1991

[54] Bolie, "Coefficients of normal blood glucose regulation", J. Appl. Physiol., 16, 1961

[55] Ackerman, Rosevar, McGuckin, "A mathematical model of the glucose-tolerance test", Phys. Med. Biol., 9, 1964

[56] Ackerman, Gatewood, Rosevar, Molnar, "Model studies of blood-glucose regulation", Bull. Math. Biophys., 27, 1965

[57] Ackerman, Gatewood, Rosevar, Molnar, "Blood Glucose Regulation and Diabetes. In: Concepts and Models of Biomathematics" , Chapter 4, F. Heinmets, ed., Marcel Dekker, 1969

[58] Cobelli, Pacini, Salvan, "On a simple model of insulin secretion", Med. & Biol. Eng. & Comput., 18, 1980

[59] Bergman, Bortolan, Cobelli, Toffolo, "Identifcation of a minimal model of glucose disappearance for estimating insulin sensitivity. In: Identifcation and System Parameter Estimation", (Proc. 5th IFAC Symposium, Darmstadt, 1979) R. Isermann, ed., Pergamon Press, Oxford, 1979

[60] Cobelli, Federspil, Pacini, Salvan, Scandellari, "An integrated mathematical model of the dynamics of blood glucose and its hormonal control", Math. Bioscien., 58, 1982

[61] Salzsieder, Albrecht, Jutzi, Fischer, "Estimation of individually adapted control parameters for an artifcial beta cell", Biomed. Biochim., 5, 1984

[62] Summers, Montani, "Mathematical model of glucose homeostasis for the study of metabolic states", J. Mississippi Acad. Sci., 34, 1989

[63] Summers, Montani, Woodward,Coleman, Hall, "Theoretical analysis of the mechanisms of chronic hyperinsulinemia", Comput. Biol. Med., 27, 1997

[64] Andreassen, Benn, Hovorka, Olesen, Carson, "A probabilistic approach to glucose prediction and insulin dose adjustment: description of metabolic model and pilot evaluation study", Comp. Meth. Prog. Biomed., 41, 1994

[65] Boroujerdi, Umpleby, Jones, Sonksen, "A simulation model for glucose kinetics and estimates of glucose utilization rate in type 1 diabetic patients", Am. J. Physiol., 268, 1995

Appendix A

Content of CD

Folder	Content
Figures	All figures included in the report.
Implementation	Matlab and simulink implementations
Report	PDF- and lyx-file of the thesis report

Table A.1: Content of CD.

Appendix B

Exogenous glucose infusion

The GIE-model models the *exogenous* glucose to be absorbed via a meal, unlike many glucose-insulin models that assumes an intravenious glucose infusion [**?**]. This models adopts the absorption model presented by Yates and Fletcher [48]. This exogenous glucose model combines a trapezoidal function describing gastric emptying, and a description of how the gut processes glucose. Yates and Fletcher define gastric emptity to have the following form [**?**]:

$$G_{empt}(t) = \begin{cases} \frac{V_{max}}{T_{asc}} \cdot t, & t < T_{asc} \\ V_{max}, & T_{asc} < t < T_{asc} + T_{max} \\ V_{max} - \frac{V_{max}}{T_{desc}} \left(t - T_{asc} - T_{max}\right), & T_{asc} + T_{max} < t \\ & < T_{asc} + T_{max} + T_{desc} \\ 0, & otherwise \end{cases} \tag{B.1}$$

All parameters are explaind in table 3.5. The parameter T_{max} is defined by the total glucose contant in a meal G_{total}, and is expressed as follows [**?**]:

$$T_{max} = \frac{G_{total} - \frac{V_{max}(T_{asc}+T_{desc})}{2}}{V_{max}} \tag{B.2}$$

The glucose dynamics G_{gut} is described by the following differential equation [**?**]:

$$\frac{dG_{gut}(t)}{dt} = G_{empt}(t) - K_{gabs}G_{gut}(t) \tag{B.3}$$

Equation B.1, B.2 and B.3 are then combined to arrive at the expression describing the exogenous glucose input [**?**]:

$$G_{exg}(t) = K_{gabs} G_{gut}(t) \tag{B.4}$$

Figure B.1 illustrates the form of the exogenous glucose input.

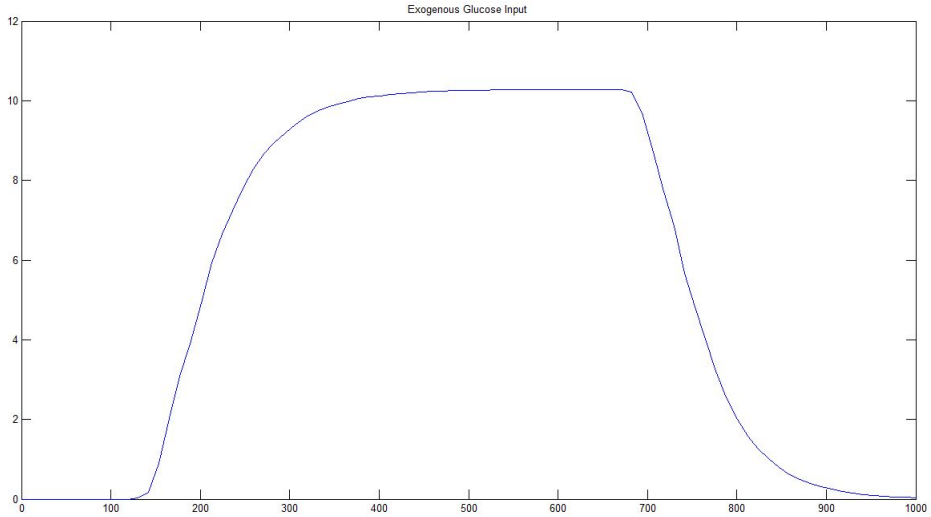

Figur B.1: Exogenous glucose input [48].

Appendix C

Model Implementation In Simulink

C.1 Input Signal

The two input signal is common in all model implementations. One signals for the glucose infusion simulating three meals over a time period of 24 hr, and a step signl infusing glucose continously to test homeostatic properties in the models. The signal are shown in figure C.1

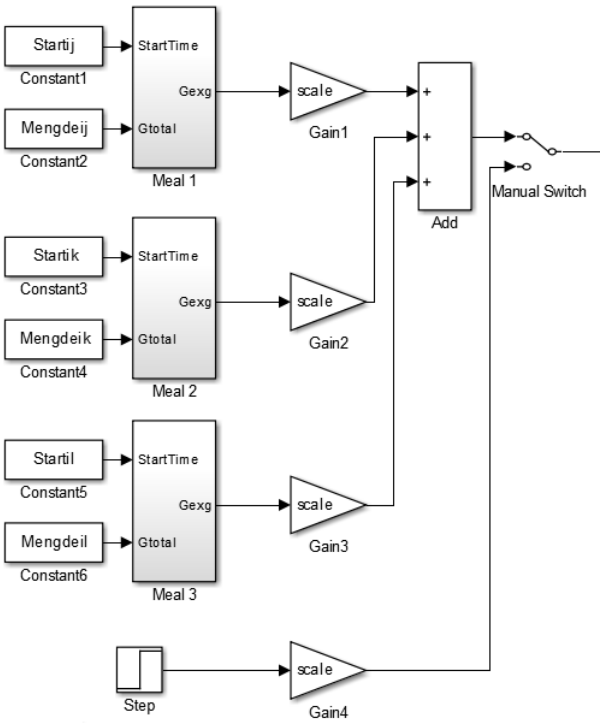

Figur C.1: Input signal common for all models.

C.2 The BMM

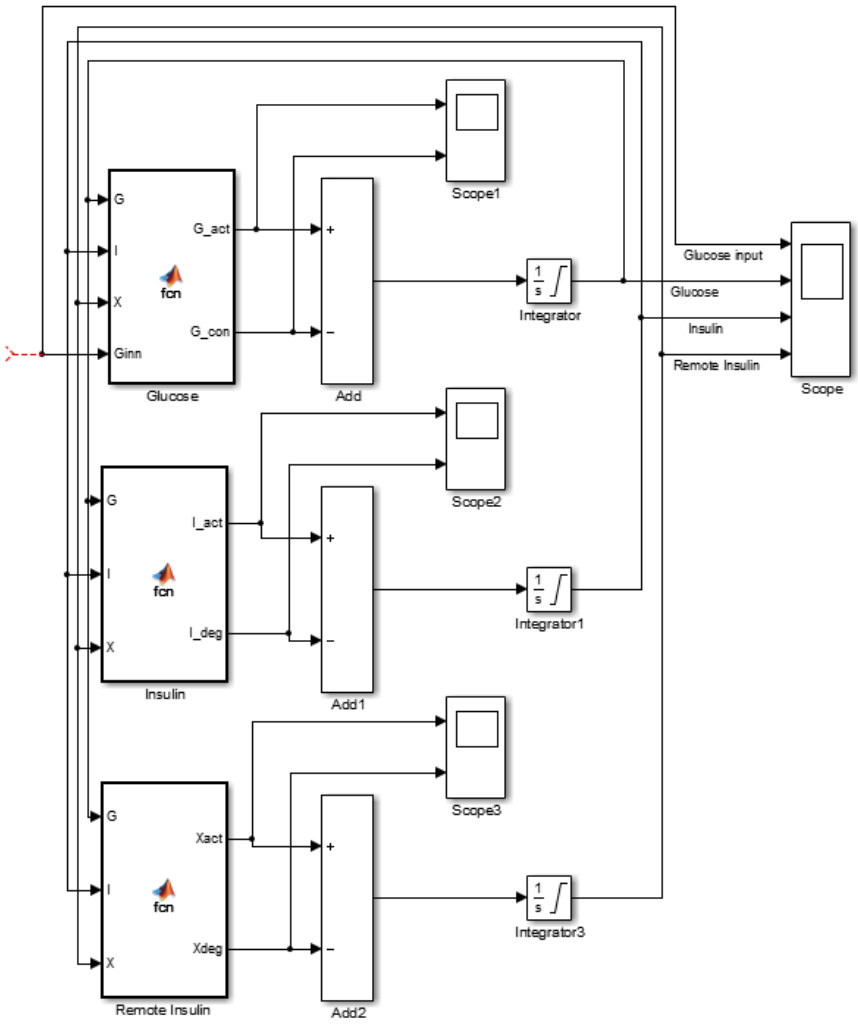

Figure C.2: Simulink implementation of the BMM-model.

C.3 The βIG-model

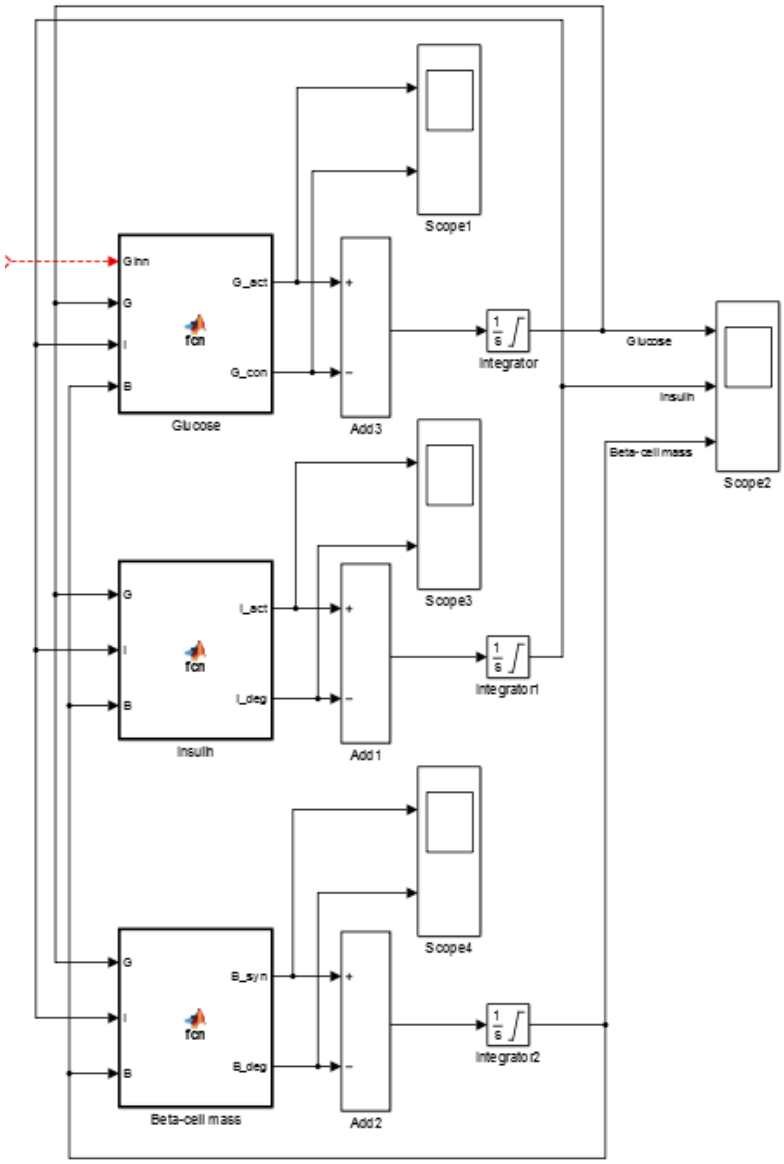

Figur C.3: Simulink implementation of the βIG-model.

C.4 The βIGIR-model

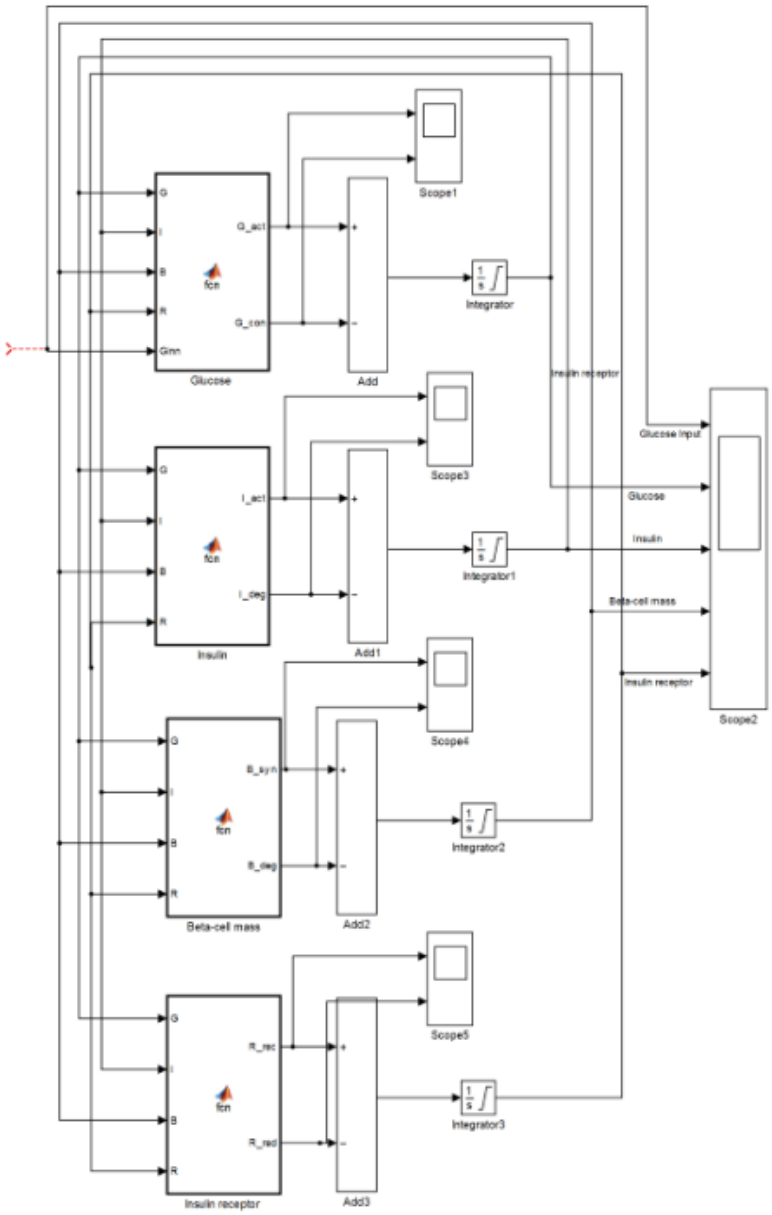

Figur C.4: Simulink implementation of the βIGIR-model.

C.5 The GIE-model

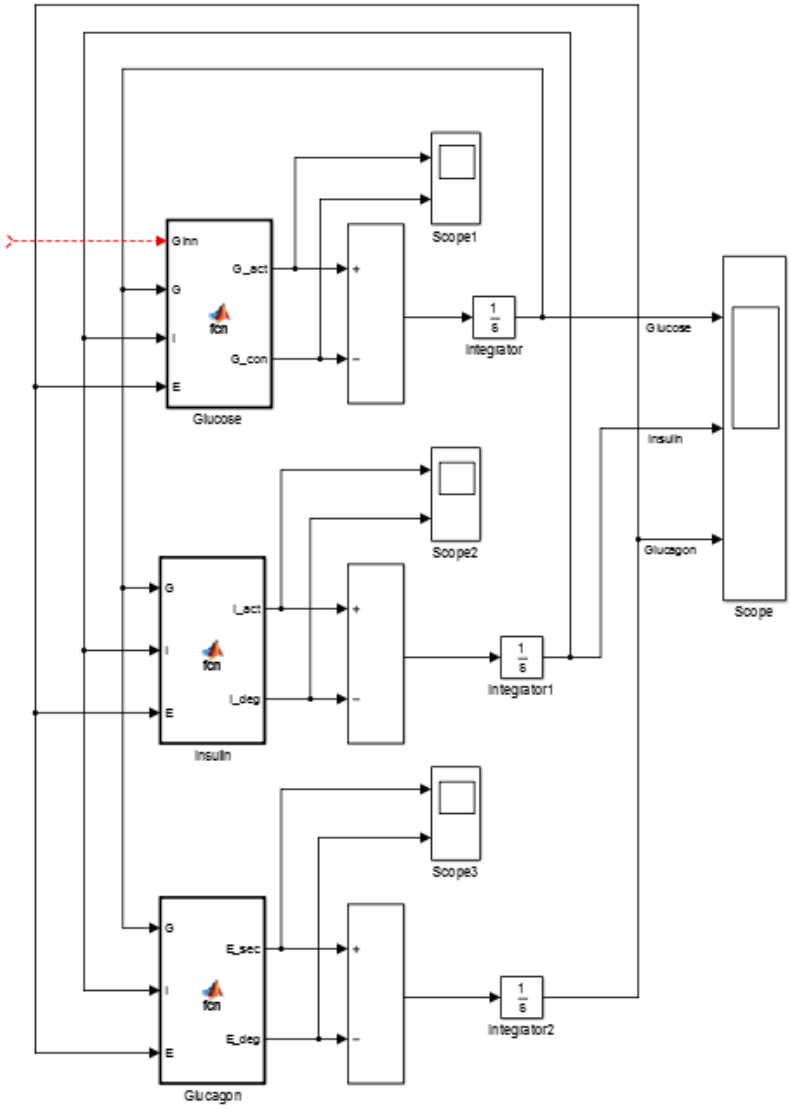

Figur C.5: Simulink implementation of the GIE-model.

C.6 The S&H-model

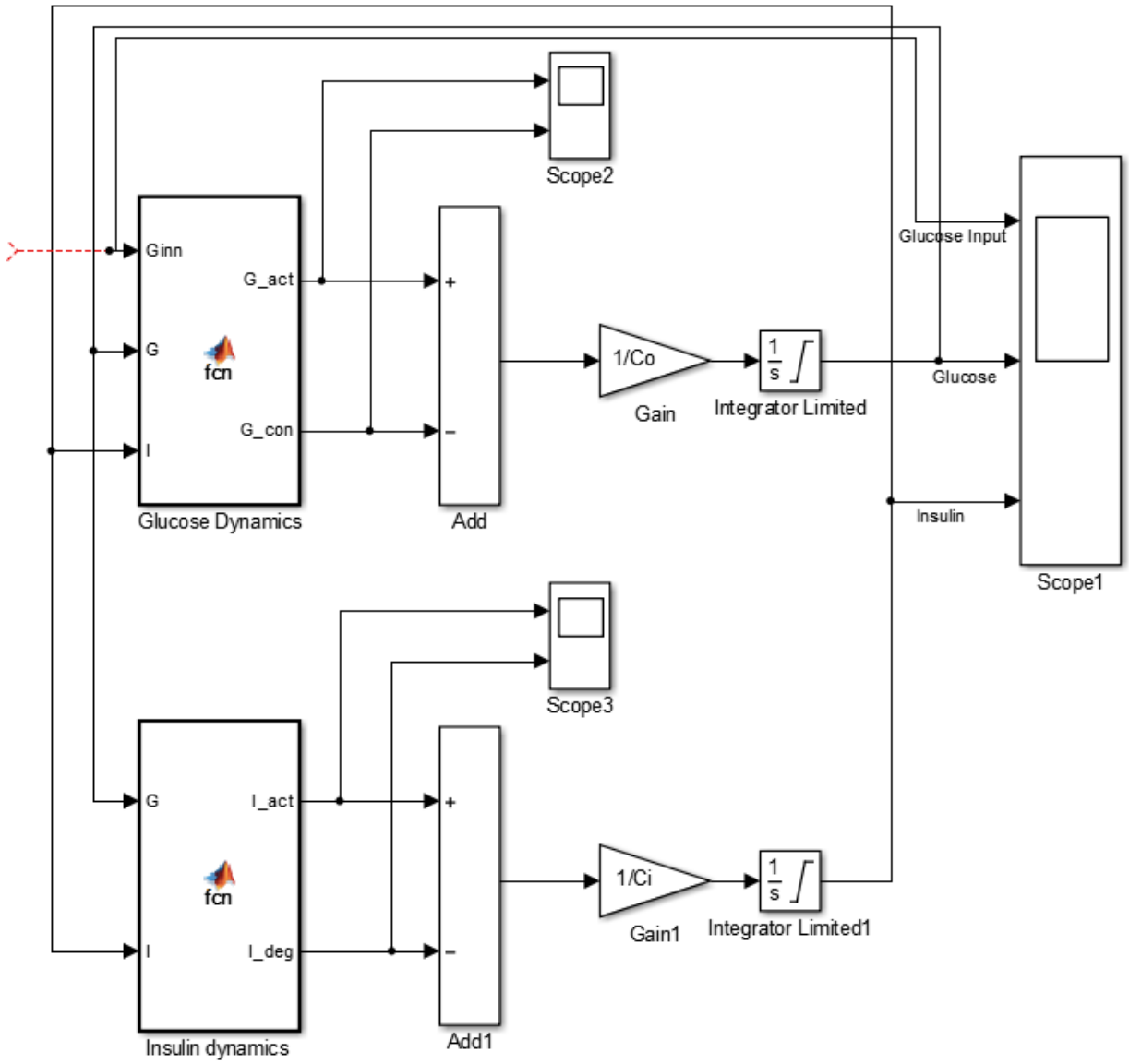

Figur C.6: Simulink implementation of the GIE-model.

Tillegg D

Source Code

D.1 Simulating And Ploting Glucose/Insulin Response

Algorithm D.1 Matlab m.file for model initiating, simulating and plotting.

```
%%
% AUTHOR    : Ingeborg Siem Kndusen
% DATE      : 03-June-2013 19:53:02
% FILENAME  : Response.m
%
% Master Thesis at The University Of Stavanger
% ----------------------------------------------------------

%Initiating Model Simulation Parameters

%The BIG-model

%Glucose Input Parameters
Tasc = 15/(24*60);        %days
Tdesc = 15/(24*60);       %days
Vmax = 360*(24*60);       %mg/days
Kgabs = (1/60)*(24*60); %days^-1

%Model Parameters
r1=8.4e-4;          %mg^-1*dl*d^-1
r2=2.4e-6;          %mg^-1*dl*d^-1
a=20000;            %mg^2*dl^-2
SI=0.72;            %muU*ml^-1*d^-1
R0=864;             %mg*dl*d^-1
Ego=1.44;           %d^-1
sigma = 432;        %muU*ml^-1*d^-1
d0 = 0.06;          %d^-1
k = 430;            %d^-1
```

Algorithm D.2 Matlab m.file for model initiating, simulating and plotting.

```
%Simulation parameters
SimTime2=1;      %Simulation Time
G2start=100;     %Glucose initial condition SS
I2start=10;      %Insulin initial condition SS
B2start=30;      %Beta-cell mass initial condition SS

%Defining Time And Quatity of
%Glucose Input

%First Meal
Start31=(1/6);
Mengde31=45e3/24;

%Second Meal
Start32=(10/24);
Mengde32=75e3/24;

%Third Meal
Start33=(17/24);
Mengde33=75e3/24;

%Simulink Simulation
sim('BIGmeal')
t1=BIG.time*24;
Glu1=BIG.signals(1,1).values; %BIG-model
Ins1=BIG.signals(1,2).values;

%%
%The BIGIR-model

%Glucose Input Parameters
Tasc = 15/(24*60);       % days
Tdesc = 15/(24*60);      % days
Vmax = 360*(24*60);      % mg/days
Kgabs = (1/60)*(24*60); % days^-1
```

Algorithm D.3 Matlab m.file for model initiating, simulating and plotting.

```
%Model Parameters
a=864;              %mg/dl d
b=1.44;             %d^-1
c=0.85;             %ml/muU d
d=43.2;             %muU/ml d mg
e=20000;            %mg^2/dl^2
f=216;              %d^-1
g=0.03;             %d^-1
h=0.5727502102e-3; %dl/mg d
i=0.2523128680e-5; %dl^2/mg^2d
j=2.64;             %d^-1
k=0.02;             %ml/muU d
l=0.24;             %d^-1

%Simulation parameters
SimTime3=1;       %Simulation Time
G3start=82;       %Glucose initial condition SS
I3start=12.70;    %Insulin initial condition SS
B3start=856.95; %Beta-cell mass initial condition SS
IRstart=0.84;     %Insulin receptor initial condition SS

%Defining Time And Quatity of
%Glucose Input

%First Meal
Start41=(1/6);
Mengde41=45e3/24;

%Second Meal
Start42=(10/24);
Mengde42=75e3/24;

%Third Meal
Start43=(17/24);
Mengde43=75e3/24;

%Simulink Simulation
sim('BIGIRmeal')
t2=BIGIR.time*24;
Glu2=BIGIR.signals(1,2).values; %BIGIR-model
Ins2=BIGIR.signals(1,3).values;
```

Algorithm D.4 Matlab m.file for model initiating, simulating and plotting.

```
%%
%GIE-Model

%Glucose Input Parameters
Tasc = 15;                  % min
Tdesc = 15;                 % min
Vmax = 360;                 % mg/min
Kgabs = 1/60;               % min^-1

%Model parameters
k1 = 1.0855*10^-4;          % min^-1 pr (ng/dl of I)
k2 = 9.7947*10^-3;          % min^-1 pr (ng/dl of I)
k3 = 207.12654;             % mg/dl
k4 = 9.1119;                % mg/dl/min
k5 = 25.3039;               % mg/dl/min
k6 = 149.7698;              % ng/dl of I
k7 = 0.4572;                % mg/dl/min
k8 = 35.3878;               % mg/dl/min
k9 = 72.9766;               % mg/dl
kr = 0.0365;                % min ^-1

Gr = 180;                   % mg/dl

a1 = 248.81;                % ng/dl/min
a2 = 0.01667;               % (mg/dl)^-1
a3 = 198;                   % mg/dl

b1 = 0.14545;               % (ng/dl/min of I) per (ng/dl
    of E)
b2 = 0.206;                 % min^-1

c0 = 0.656;                 % ng/dl/min
c1 = 2.5441;                % (ng/dl/min of E) per (mg/dl
    of G)
c2 = -5.2523;               % ng/dl (of I)
c3 = 0.08;                  % min^-1

Ge = 75;                    % mg/dl

%Simulation parameters
SimTime5=1440;          %Simulation Time
G5start = 93.6;         %Glucose initial condition SS
I5start = 41.6;         %Insulin initial condition SS
E5start = 8.2;          %Glucagon initial condition SS
```

Algorithm D.5 Matlab m.file for model initiating, simulating and plotting.

```
%Defining Time And Quatity of
%Glucose Input

%First Meal
Start21=240;
Mengde21=45e3;

%Second Meal
Start22=600;
Mengde22=75e3;

%Third Meal
Start23=1020;
Mengde23=75e3;

%Simulink Simulation
sim('GIEmeal');
t3=GIE.time/60;
Glu3=GIE.signals(1,1).values;    %GIE-model
Ins3=GIE.signals(1,2).values/4;

%%
%SogH-model

%Glucose Input Parameters
Tasc = 15/60;   %hr
Tdesc = 15/60;  %hr
Vmax = 360*60;  %mg/hr
Kgabs = 60/60;  %hr-1

%Model Parameters
gamma=13.9;       %mg*hr^-1*mg%^-1*mU%^-1
Gt=0;             %mg%
delta=24.7;       %mUhr^-1*mg%
my=72;            %mg*hr^-1*mg%^-1
Gk=250;           %mg%
alpha=76;         %mUhr^-1*mU%^-1
beta=14.3;        %mUhr^-1mg%^-1
G0=51;            %mg%
Co = 150;         %dl
Ci = 150;         %mU/mU
```

Algorithm D.6 Matlab m.file for model initiating, simulating and plotting.

```
%Simulation parameters
SimTime4=24;     %Simulation Time
G4start=90;      %Glucose initial condition SS
I4start=7.4;     %Insulin initial condition SS

%Defining Time And Quatity of
%Glucose Input

%First Meal
Start1=4;
Mengde1=45e3;

%Second Meal
Start2=10;
Mengde2=75e3;

%Third Meal
Start3=17;
Mengde3=75e3;

%Simulink Simulation
sim('SandHMeal')
t4=SandH.time;
Glu4=SandH.signals(1,2).values; %S&H-model
Ins4=SandH.signals(1,3).values;

%%
%The GIM-model

load('GIM2.mat')
t5=Time/60;
Glu5=Glucose;          %GIM-model
Ins5=Insulin/6.9450; %Convert [pmol/l] to [muU/ml]

%%
%Creating Comparative Glucose Plot

clear figure(1)
figure(1)

plot(t1,Glu1,'g',t2,Glu2,'b',t3,Glu3,'y',t4,Glu4,'k',t5
    ,Glu5,'r');
title('Glucose Response Of The Glucoregulatory Models')
ylabel('Glucose Consentration [mg/dl]')
xlabel('Time [hr]')
legend('The BIG-model',...
          'The BIGIR-model','The GIE-model',...
          'The S&H-model','The GIM-model (reference)');
```

Algorithm D.7 Matlab m.file for model initiating, simulating and plotting.

```
%%
%Creating Comparative Insulin Plot

clear figure(2)
figure(2)

plot(t1,Ins1,'g',t2,Ins2,'b',t3,Ins3,'y',t4,Ins4,'k',t5
    ,Ins5,'r');
title('Insulin Response Of The Glucoregulatory Models')
ylabel('Insulin Consentration [  \muU/ml]')
xlabel('Time [hr]') legend('The BIG-model',...
          'The BIGIR-model','The GIE-model',...
          'The S&H-model','GIM-model (reference)');
```

D.2 Simulating And Ploting "Homeostasis Test"

Algorithm D.8 Matlab m.file for model initiating, simulating and plotting.

```
%%
% AUTHOR    : Ingeborg Siem Kndusen
% DATE      : 03-June-2013 19:53:02
% FILENAME  : Homeo.m
%
% Master Thesis at The University Of Stavanger
%
%%-----------------------------------------------------------

%Initiating Model Simulation Parameters


%The BIG-Model

%Glucose step
Start2=4/24;      %day
Stopp2=20/24;     %day
Init2=0;
Value2=1e4;       %day

%Model Parameters
r1=8.4e-4;        %mg^-1*dl*d^-1
r2=2.4e-6;        %mg^-1*dl*d^-1
a=20000;          %mg^2*dl^-2
SI=0.72;          %muU*ml^-1*d^-1
R0=864;           %mg*dl*d^-1
Ego=1.44;         %d^-1
sigma = 432;      %muU*ml^-1*d^-1
d0 = 0.06;        %d^-1
k = 430;          %d^-1
```

Algorithm D.9 Matlab m.file for model initiating, simulating and plotting.

```
%Simulation parameters
SimTime2=1;       %Simulation time
G2start=100;      %Glucose initial condition SS
I2start=10;       %Insulin initial condition SS
B2start=30;       %Beta-cell mass initial condition SS

%%
%The BIGIR-Model

%Glucose step
Start3=4/24;      %day
Stopp3=20/24;     %day
Init3=0;
Value3=1e4;       %day

%Model Parameters
a=864;            %mg/dl d
b=1.44;           %d^-1
c=0.85;           %ml/muU d
d=43.2;           %muU/ml d mg
e=20000;          %mg^2/dl^2
f=216;            %d^-1
g=0.03;           %d^-1
h=0.5727502102e-3; %dl/mg d
i=0.2523128680e-5; %dl^2/mg^2d
j=2.64;           %d^-1
k=0.02;           %ml/muU d
l=0.24;           %d^-1

%Simulation parameters
SimTime3=1;       %Simulation Time
G3start=82;       %Glucose initial condition SS
I3start=12.70;    %Insulin initial condition SS
B3start=856.95;   %Beta-cell mass initial condition SS
IRstart=0.84;     %Insulin receptor initial condition SS
```

Algorithm D.10 Matlab m.file for model initiating, simulating and plotting.

```
%%
%The S&H-model

%Glucose step
Start4=4;    %hr
Stopp4=20;   %hr
Init4=0;
Value4=1e4; %hr

%Model Parameters
gamma=13.9; %mg*hr^-1*mg%^-1*mU%^-1
Gt=0;        %mg%
delta=24.7; %mUhr^-1*mg%
my=72;       %mg*hr^-1*mg%^-1
Gk=250;      %mg%
alpha=76;    %mUhr^-1*mU%^-1
beta=14.3;   %mUhr^-1mg%^-1
G0=51;       %mg%
Co = 150;    %dl
Ci = 150;    %mU/mU

%Simulation parameters
SimTime4=24;%Simulation time
G4start=90; %Glucose initial condition SS
I4start=7.4;%Insulin initial condition SS

%%
%The GIE-model

%Glucose step
Start5=4*60;          %min
Stopp5=20*60;         %min
Init5=0;
Value5=1e4/60;        %min
```

Algorithm D.11 Matlab m.file for model initiating, simulating and plotting.

```
%Model parameters
k1 = 1.0855*10^-4;  % min^-1 pr (ng/dl of I)
k2 = 9.7947*10^-3;  % min^-1 pr (ng/dl of I)
k3 = 207.12654;     % mg/dl
k4 = 9.1119;        %mg/dl/min
k5 = 25.3039;       % mg/dl/min
k6 = 149.7698;      % ng/dl of I
k7 = 0.4572;        % mg/dl/min
k8 = 35.3878;       % mg/dl/min
k9 = 72.9766;       %mg/dl

kr = 0.0365;        % min ^-1
Gr = 180;           % mg/dl

a1 = 248.81;        % ng/dl/min
a2 = 0.01667;       % (mg/dl)^-1
a3 = 198;           % mg/dl

b1 = 0.14545;       % (ng/dl/min of I) per (ng/dl of E)
b2 = 0.206;         % min^-1

c0 = 0.656;         % ng/dl/min
c1 = 2.5441;        % (ng/dl/min of E) per (mg/dl of G)
c2 = -5.2523;       % ng/dl (of I)
c3 = 0.08;          % min^-1

Ge = 75;            % mg/dl

%Simulation parameters
SimTime5=1440;      %Simulation Time
G5start = 93.6;     %Glucose initial condition SS
I5start = 41.6;     %Insulin initial condition SS
E5start = 8.2;      %Glucagon initial condition SS
```

Algorithm D.12 Matlab m.file for model initiating, simulating and plotting.

```
%%
%Simulating The Models In Simulink

sim('BIGhomeo');
sim('BIGIRhomeo');
sim('GIEhomeo');
sim('SandHhomeo');

%Creating The Time Vectors
t1=BIG.time*24;      %hr
t2=BIGIR.time*24;    %hr
t3=GIE.time/60;      %hr
t4=SandH.time;       %hr

%Extracting Glucose And Insulin Values
Glu1=BIG.signals(1,1).values;    %BIG-model
Ins1=BIG.signals(1,2).values;

Glu2=BIGIR.signals(1,2).values; %BIGIR-model
Ins2=BIGIR.signals(1,3).values;

Glu3=GIE.signals(1,1).values;    %GIE-model
Ins3=GIE.signals(1,2).values/4;

Glu4=SandH.signals(1,2).values; %S&H-model
Ins4=SandH.signals(1,3).values;
```

Algorithm D.13 Matlab m.file for model initiating, simulating and plotting.

```
%%
%Creating Comparative Glucose Plot

clear figure(1)
figure(1)

plot(t1,Glu1,'g',t2,Glu2,'b',t3,Glu3,'r',t4,Glu4,'k');
title('Glucose Dynamics Of The Glucoregulatory Models')
ylabel('Glucose Consentration [mg/dl]')
xlabel('Time [hr]')
legend('The BIG-model',...
        'The BIGIR-model','The GIE-model',...
        'The S&H-model');

%%
%Creating Comparative Insulin Plot

clear figure(2)
figure(2)

plot(t1,Ins1,'g',t2,Ins2,'b',t3,Ins3,'r',t4,Ins4,'k');
title('Insulin Dynamics Of The Glucoregulatory Models')
    ;
ylabel('Insulin Consentration [  \muU/ml]');
xlabel('Time [hr]')
legend('The BIG-model',...
        'The BIGIR-model','The GIE-model',...
        'The S&H-model');
```